Sr isotopes in arcs revisited: tracking slab dehydration using $\delta^{88/86}$Sr and ^{87}Sr/^{86}Sr systematics of arc lavas

Martijn Klaver[1,2]*, Jamie Lewis[1], Ian J. Parkinson[1], Marlina A. Elburg[3], Pieter Z. Vroon[4], Katherine A. Kelley[5] and Tim Elliott[1]

[1]Bristol Isotope Group, School of Earth Sciences, University of Bristol; Wills Memorial Building, Queen's Road, Bristol BS8 1RJ, United Kingdom

[2]School of Earth and Ocean Sciences, Cardiff University; Main Building, Park Place, Cardiff CF10 3AT, United Kingdom

[3]Department of Geology, University of Johannesburg; PO Box 524, Auckland Park 2006, South Africa

[4]Faculty of Science, Vrije Universiteit Amsterdam; De Boelelaan 1085, 1081HV Amsterdam, Netherlands

[5]Graduate School of Oceanography, University of Rhode Island; Narragansett Bay Campus, Narragansett, RI 02882, United States

*corresponding author: klaverm@cardiff.ac.uk

ABSTRACT

Dehydration of the subducting slab is a crucial process in the generation of hydrous convergent margin magmas, yet the exact processes of how and where the slab dehydrates and how these fluids are transported to the mantle wedge remain obscure. Strontium is a "fluid-mobile" element and as such well suited to investigate the source of slab-derived fluids. We employ mass-dependent Sr isotope systematics ($\delta^{88/86}$Sr; the deviation in ^{88}Sr/^{86}Sr of a sample relative to NIST SRM 987) of primitive arc lavas, in tandem with conventional radiogenic ^{87}Sr/^{86}Sr measurements, as a novel tracer of slab dehydration.

To characterise the $\delta^{88/86}$Sr composition of subduction zone inputs, we present new $\delta^{88/86}$Sr data for subducting sediments, altered oceanic crust and MORB. Calcareous sediments are isotopically lighter and carbonate-free sediments are isotopically heavier than mid-ocean ridge basalts (MORB). Samples of the altered oceanic crust display elevated ^{87}Sr/^{86}Sr but only the most intensely altered sample has significantly higher $\delta^{88/86}$Sr than pristine MORB. Mafic arc lavas from the Aegean and Mariana arc invariably have a mass-dependent Sr isotope composition that is indistinguishable from MORB and lower ^{87}Sr/^{86}Sr than upper altered oceanic crust. This $\delta^{88/86}$Sr-^{87}Sr/^{86}Sr signature of the arc lavas, in combination with their high but variable Sr/Nd, can only be explained if it is provided by a fluid that acquired its Sr isotope signature in the deeper, less altered part of the subducted oceanic crust. We propose a model where the breakdown of serpentinite in the slab mantle releases a pulse of fluid at sub-arc depths. These fluids travel through and equilibrate with the overlying oceanic crust and induce wet partial melting of the upper altered crust and sediments. This hydrous melt is then delivered to the mantle source of arc magmas as a single metasomatic component.

From mass balance it follows that the slab-derived fluid contributes >70 % of the Sr budget of both Mariana and Aegean arc lavas. Whereas this fluid-dominated character is unsurprising for the sediment-poor Mariana arc, the Aegean arc sees the subduction of 3-6 km of calcareous sediments that were found to exert very little control on the Sr budget of the arc magmas and are overwhelmed by the fluid contribution.

KEYWORDS: mass-dependent Sr isotope variations; arc magmatism; serpentinite fluid; subducting sediment; altered oceanic crust

1. Introduction

A geochemical signature of recycled oceanic crust and its sedimentary cover is one of the hallmarks of magmas erupted at convergent margins. Strong evidence for the rapid recycling of sediments from the slab to arc front volcanoes comes from above-background ^{10}Be abundances in arc lavas (Tera et al., 1986) and the global correlation of subducted sediment fluxes with the volcanic outputs for trace elements (Plank and Langmuir, 1993). In addition, the Pb isotope composition of island arc basalts typically reflects the isotope composition of subducting sediments (e.g., White and Dupré, 1986; Vroon et al., 1995; Turner et al., 1997).

The addition of a sediment component to the mantle source of island arc basalts, either as a partial melt or by bulk addition, cannot account for all trace element and isotopic characteristics of arc lavas (see Elliott, 2003). Island arc basalts commonly display notable excesses in the abundance of 2+ cations (Sr, Ba, Pb) and other "fluid-mobile" elements compared to elements of similar magmatic compatibility. This distinct geochemical signature, together with ^{238}U excesses, elevated B contents and high δ^{11}B, points to the contribution of a fluid component (Gill and Condomines, 1992; Ryan and Langmuir, 1993; Ishikawa and Nakamura, 1994). The exact nature and origin of the fluid component are, however, controversial. The fluid component has traditionally been inferred to derive from dehydration of the upper, altered part of the oceanic crust (Hawkesworth et al., 1977; Miller et al., 1994; Elliott et al., 1997; Turner et al., 1997) but there are several complications to this model. Combining thermal modelling with experimentally determined stability fields of hydrous phases indicates that dehydration of the upper part of the slab is mostly achieved in the forearc and little of its water is released at sub-arc depths (e.g., Schmidt and Poli, 1998; van Keken et al., 2011; Spandler and Pirard, 2013). In addition, there is a pronounced Sr and Pb isotope mismatch between the fluid component recorded in island arc basalts and the composition of altered oceanic crust (e.g., Class et al., 2000; Elliott, 2003; Avanzinelli et al., 2012; Freymuth et al., 2015).

An alternative interpretation that has recently gained in popularity is that the sedimentary cover physically mixes with peridotite at the slab-wedge interface to form a mélange (Marschall and Schumacher, 2012; Nielsen and Marschall, 2017). Subsequent partial melting of such a mélange in the presence of residual accessory phases is argued to generate the characteristic trace element decoupling of arc lavas, including their positive 2+ cation anomalies. Of particular relevance is that the mélange model promotes an explanation for the ^{87}Sr/^{86}Sr-^{143}Nd/^{144}Nd systematics and high Sr/Nd of arc lavas without the need for a separate fluid contribution (Nielsen and Marschall, 2017).

We investigate the use of mass-dependent Sr isotope systematics in understanding the mechanisms of mass transport from the slab to the mantle wedge. Strontium is a suitable element for such a study as it offers a double isotope perspective in which mass-dependent Sr isotope systematics ($\delta^{88/86}$Sr) can be combined with conventional radiogenic ^{87}Sr/^{86}Sr. Measurements of mass-dependent Sr isotope variation provide a novel tracer of high-temperature geochemical and cosmochemical processes (Moynier et al., 2010; Charlier et al., 2012; Charlier et al., 2017; Amsellem et al., 2018). There is no previous systematic study of $\delta^{88/86}$Sr in arc lavas, yet evident promise lies in the known variability of $\delta^{88/86}$Sr in recycled components. Whereas these all have higher ^{87}Sr/^{86}Sr than depleted mantle, $\delta^{88/86}$Sr of oceanic crust and its sedimentary cover potentially displays a much greater variation, extending to both isotopically heavier (higher $\delta^{88/86}$Sr) and lighter (lower $\delta^{88/86}$Sr) values than mid-ocean ridge basalts. Carbonate-rich sediments are isotopically lighter while seawater is isotopically heavier than mantle values (Krabbenhöft et al., 2010; Pearce et al., 2015; Stevenson et al., 2016). An experimental study found that the Sr isotope composition of basalt becomes heavier during interaction with seawater at 250-290 °C (Voigt et al., 2018), which suggests that altered oceanic crust may have higher $\delta^{88/86}$Sr than pristine MORB. Hence, combining radiogenic and mass-dependent Sr isotope variations can contribute to disentangling the contributions of these components to the Sr budget of arc magmas.

For this study, we have measured a suite of well-characterised mafic lavas from the Mariana and Aegean arcs for their ^{87}Sr/^{86}Sr and $\delta^{88/86}$Sr isotope composition. These arcs are situated towards either end of the global spectrum of arc basalts that has traditionally been interpreted as sediment-poor to sediment-dominated arcs (Figure 1). Hence, these samples are ideally suited not only to investigate the potential source of slab-derived fluids (Mariana arc), but also the leverage that subducted sediments have on the Sr budget of arc magmas

(Aegean arc). A notable fraction of Aegean arc lavas has very high Sr contents, ranging up to 1070 µg/g Sr in some primitive lavas in the Eastern section of the arc (Francalanci et al., 1995; Spandler et al., 2012; Elburg et al., 2014; Elburg et al., 2018; Klaver et al., 2018). The sediment pile on the subducting plate at the Aegean trench (8 km) is globally amongst the thickest (Clift and Vannucchi, 2004), compared to <500 m in the Mariana arc (Plank and Langmuir, 1998), and 40-80 % of incoming sediment is subducted rather than accreted (Kopf et al., 2003). In addition, subducting sediment in the Aegean is unusually rich in carbonate (Klaver et al., 2015), which could affect the composition of the arc lavas (Woelki et al., 2018) and form a possible source for the high Sr contents of Aegean arc lavas. To further constrain the $\delta^{88/86}$Sr composition of recycled components and the depleted mantle, we have measured the composition of subducting sediment in the Aegean and Mariana arcs, as well as five normal mid-ocean ridge basalt (N-MORB) glasses and nine altered oceanic crust composite samples from ODP site 801 directly east of the Mariana arc.
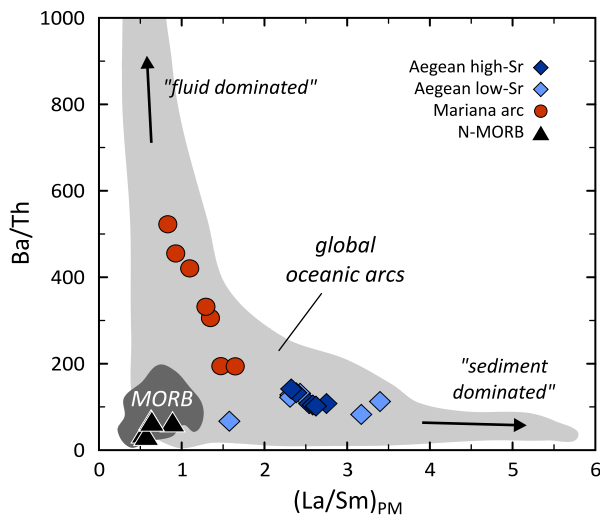

Figure 1. *La/Sm (primitive mantle-normalised; Sun and McDonough, 1989) versus Ba/Th diagram with the Aegean arc and Mariana arc samples measured in this study. Global oceanic arcs (see supplementary Dataset 2) show a variation that is commonly interpreted as ranging from sediment-dominated to sediment-poor, fluid-dominated arcs (Elliott, 2003). Primitive Aegean arc samples display a bimodal distribution of Sr contents and are hence divided in a low-Sr (<600 µg/g) and high-Sr (>900 µg/g) suite. Black triangles are the N-MORB samples measured for $\delta^{88/86}$Sr in this study.*

2. Samples and methods

2.1. Samples

This study uses samples from the Aegean and Mariana arcs that have been well-characterised for their major element, trace element and radiogenic isotope compositions (Elliott et al., 1997; Elburg et al., 2014; Klaver et al., 2016; Klaver et al., 2018). On the global spectrum (Figure 1a), the Mariana arc is fluid-dominated with only a relatively small contribution from subducting sediment as indicated by many samples with high Ba/Th, large ^{238}U excesses but low La/Sm and radiogenic ^{143}Nd/^{144}Nd (e.g., Elliott et al., 1997). Aegean arc lavas, in contrast, display a strong signature of recycled sediment, as indicated by high La/Sm, Th/Nb and unradiogenic ^{143}Nd/^{144}Nd (e.g., Bailey et al., 2009; Elburg et al., 2014; Klaver et al., 2016; Elburg and Smet, 2020). To minimise potential effects of magma differentiation on mass-dependent Sr isotope systematics, the most mafic samples of each locality were selected. Several Aegean andesites to rhyodacites were also included to specifically assess the influence of crustal processes. Primitive Aegean arc lavas, mainly from Nisyros volcano, have Mg# (molar Mg/[Mg+Fe]) >55 and low phenocryst contents. Plagioclase is a common groundmass phase but rarely occurs as phenocrysts. By contrast, the Mariana samples are more phyric, contain plagioclase pheno- and antecrysts and are slightly more evolved (Mg# 45-55).

Sediment samples recovered from DSDP/ODP sites in the eastern Mediterranean Sea (hereafter referred to as "Aegean sediments") and western Pacific Ocean (hereafter referred to as "Mariana sediments") were analysed to constrain the Sr isotope composition of local subducting sediments. A description and geochemical characterisation of the Aegean sediment samples is given by Klaver et al. (2015). Aegean sediments are binary mixtures of Sahara dust and Nile-derived detritus diluted by up to 60 % carbonate, which dominates their Sr budget (Weldeab et al., 2002; Klaver et al., 2015). The measured sediment samples include two compositional

extremes and a sample from a mud volcano (ODP site 971B) that represents a natural composite of Eocene to middle Miocene sediments below the Mediterranean evaporite seal. Two samples of these Messinian evaporites were also measured for their Sr isotope composition.

Mariana sediment samples from ODP site 801 (leg 129) comprise the entire sedimentary cover of the Pacific plate directly east of the Mariana arc. The dominant lithologies are Cenozoic pelagic clays and chert, Cretaceous volcaniclastic turbidites with an ocean island basalt affinity and Jurassic radiolarite with variable proportions of claystone (Lancelot et al., 1990). Geochemical characterisation of these lithological units is provided by Karl et al. (1992), Karpoff (1992), Elliott et al. (1997) and Plank and Langmuir (1998). A representative sample of each unit has been measured for its Sr isotope composition in this study. Mariana sediments were deposited below the carbonate compensation depth (CCD) and contain very little carbonate, in clear contrast with the calcareous nature of the Aegean sediments.

Site 801 was deepened during ODP leg 185 to penetrate the extrusive section of the ~170 Ma Pacific oceanic crust (Plank et al., 2000). High recovery of the mafic crust allows high-resolution geochemical characterisation, but we use the composite samples of Kelley et al. (2003) as more representative average compositions of the altered oceanic crust (AOC). These composites were made by physical mixing of sample powders of the lithologies present in the depth intervals 0-110 m, 110-220 m and 220-420 m in the extrusive section of the oceanic crust. For each depth interval, three composites were available, following the approach pioneered by Staudigel et al. (1995). Composites labelled "VCL" (volcaniclastic) are biased towards more altered, brecciated material and "FLO" (flows) are biased to less altered extrusive lava compositions, whereas composites labelled "ALL" represent a weighted average of all lithologies. See Kelley et al. (2003) for a detailed description of the AOC composite samples.

To constrain the mass-dependent Sr isotope composition of the depleted mantle, five N-MORB glasses were included in this study. Well-characterised, mafic (≥7.5 wt.% MgO, >100 µg/g Ni) samples with primitive mantle-normalised (Sun and McDonough, 1989) La/Sm <1 were selected from a suite of MORB samples. Two samples from the East Pacific Rise (9°28' to 9°52' N) are taken from the glassy margins of lava flows collected by submersible within two years of emplacement (Rubin et al., 1994; Sims et al., 2002). Three additional samples have not been dated but were dredged from the axial graben at 26° S along the Mid-Atlantic Ridge (Niu and Batiza, 1994) and 66° E along the Southwest Indian Ridge (Robinson et al., 1996). More detailed summaries of locations and the samples are provided by Marschall et al. (2017). The MORB samples were gently crushed by hand after which clean glass shards were handpicked with the aid of a binocular microscope, taking care to exclude any fragments with inclusions or alteration. The glass chips were cleaned in an ultrasonic bath in methanol and 18.2 MΩ·cm water prior to further processing.

2.2. Analytical techniques

Mass-dependent Sr isotope compositions ($\delta^{88/86}$Sr) were determined using the double spike technique employing an ^{87}Sr-^{84}Sr double spike (Lewis et al., 2017). Due to the natural variability in radiogenic ^{87}Sr/^{86}Sr, two separate measurements are required for each sample; the unspiked sample for the radiogenic measurement and a measurement of a spiked aliquot. Although yields of the chemical purification procedure were very high, aliquots of the samples were spiked prior to processing to eliminate the effects of any potential fractionation caused by non-quantitative recovery of Sr through the Sr purification procedure.

Sample powders were digested in 3:1 concentrated HF and HNO_3 at 140 °C for four days. After evaporation of the acid, the residues were treated with concentrated HNO_3 twice and subsequently dissolved in 3 M HNO_3. An aliquot of the sample, corresponding to 200 ng Sr, was equilibrated with 100 ng of the ^{87}Sr-^{84}Sr double spike overnight. Spiked and unspiked aliquots were processed using separate sets of columns and PFA beakers to prevent contamination of the radiogenic measurements with the double spike, but otherwise identical procedures were followed. Strontium was separated from the matrix using Eichrom Sr specific resin (Horwitz et al., 1992) where Sr is selectively retained on the column in 3 M HNO_3 while matrix elements are eluted. Strontium is subsequently recovered with 18.2 MΩ·cm water. The Sr fractions are evaporated to dryness together with 50 µL 0.2 % H_3PO_4 and treated with concentrated HNO_3 twice to eliminate any residual organic material. Total

procedural blanks were <20 pg Sr and thus negligible compared to the amount of Sr processed for the measurements (≥300 ng).

The Sr fractions were loaded onto degassed annealed Re filaments together with a $TaCl_5$ activator. Measurements were performed using a Thermo Finnigan Triton TI thermal ionisation mass spectrometer (TIMS), equipped with 10^{11} Ω amplifiers, using a multi-dynamic routine to cancel out cup efficiency and gain factors (see supplementary material for more details). Data were acquired in 10 blocks of 20 cycles of 4.2 s integration time with 6 s idle time between magnet jumps. Isobaric interference of ^{87}Rb was monitored at mass 85; the $^{85}Rb^+$ ion beam intensity was always <0.01 pA and hence corrections were trivial. Radiogenic Sr data ($^{87}Sr/^{86}Sr$) were corrected for instrumental mass fractionation to $^{86}Sr/^{88}Sr$ = 0.1194 (Nier, 1938). The magnitude of natural mass-dependent Sr isotope fractionation was calculated offline following the numerical double spike inversion approach of Rudge et al. (2009) using the measured radiogenic isotope composition of the samples. Mass-dependent Sr isotope composition data are reported relative to NIST SRM 987 as $\delta^{88/86}Sr_{SRM\ 987}$ (hereafter abbreviated to $\delta^{88/86}Sr$) following the definition of Coplen (2011). Reported uncertainties in Table 1 are the 2 standard error measurement precision ($2s_{\bar{x}}$). Aliquots of NIST SRM 987 processed through the chemical purification procedure yield $^{87}Sr/^{86}Sr$ = 0.710248 ± 0.000010 and $\delta^{88/86}Sr$ = 0.004 ± 0.014 ‰ (2s, n = 13), indicating that no bias is introduced during sample processing that is not corrected for by the double spike. Repeated measurements of USGS reference materials BHVO-2 (basalt) and RGM-1 (rhyolite) yield $^{87}Sr/^{86}Sr$ = 0.703476 ± 0.000007, $\delta^{88/86}Sr$ = 0.267 ± 0.010 ‰ (2s, n = 6) and $^{87}Sr/^{86}Sr$ = 0.704195 ± 0.000007, $\delta^{88/86}Sr$ = 0.196 ± 0.014 ‰ (2s, n = 5), respectively (see supplementary Figure S1). The pooled 2s intermediate precision for these three reference materials is 0.013 ‰, which we take as the best estimate of the uncertainty on our $\delta^{88/86}Sr$ measurements.

3. Results

The $^{87}Sr/^{86}Sr$ and $\delta^{88/86}Sr$ data for the arc lavas, subducting sediments, altered oceanic crust and N-MORB samples are given in Table 1 and shown in Figure 2. New $^{87}Sr/^{86}Sr$ data agree well with previously published values (see supplementary Figure S2). The five N-MORB glasses yield $\delta^{88/86}Sr$ between 0.252 and 0.300 ‰ with an average of 0.279 ± 0.039 ‰ (2s). Composite AOC samples display a range in $^{87}Sr/^{86}Sr$ and $\delta^{88/86}Sr$ of 0.7032 to 0.7079 and 0.264 to 0.340 ‰, respectively. The VCL composites, which are biased towards more altered volcaniclastic material, have the highest $^{87}Sr/^{86}Sr$ for each depth interval, whereas the FLO composites, biased to less altered flows, have the lowest $^{87}Sr/^{86}Sr$. Only the 0-110 m VCL composite has significantly higher $\delta^{88/86}Sr$ than MORB. The weighted average composition of the upper AOC at ODP site 801 is $^{87}Sr/^{86}Sr$ = 0.7042 and $\delta^{88/86}Sr$ = 0.270 ‰ (Table 1).

Primitive Mariana and Aegean arc lavas display limited variation in $\delta^{88/86}Sr$ (0.263-0.305 ‰) that is indistinguishable from N-MORB. In the Mariana sample set, the two samples from Guguan have marginally higher $\delta^{88/86}Sr$ compared to the other five samples. The average $\delta^{88/86}Sr$ for the Mariana samples is 0.283 ± 0.029 ‰ (2s, n = 7). The Aegean primitive samples are homogeneous with an average $\delta^{88/86}Sr$ of 0.283 ± 0.020 ‰ (2s, n = 15). There is no significant difference in $\delta^{88/86}Sr$ between Aegean lavas with Sr contents <600 µg/g (low-Sr suite) and Sr contents >900 µg/g (high-Sr suite) in $\delta^{88/86}Sr$, although the latter have lower $^{87}Sr/^{86}Sr$. Andesitic to rhyodacitic Aegean samples (evolved suite) have lighter Sr isotope compositions ($\delta^{88/86}Sr$ = 0.207-0.255) than the primitive samples.

Calcareous Aegean sediments have $\delta^{88/86}Sr$ = 0.195-0.213 ‰, isotopically lighter than the N-MORB and mafic arc samples, but the two Messinian evaporite samples have amongst the highest $\delta^{88/86}Sr$ found in terrestrial rocks (0.460 and 0.606 ‰). All Aegean sediments have $^{87}Sr/^{86}Sr$ around the value of Neogene seawater (~0.709). The carbonate-poor Mariana sediments display a much greater variability in $^{87}Sr/^{86}Sr$ (0.7065-0.7181) but have mass-dependent Sr isotope compositions between that of MORB and seawater (0.318-0.382 ‰).
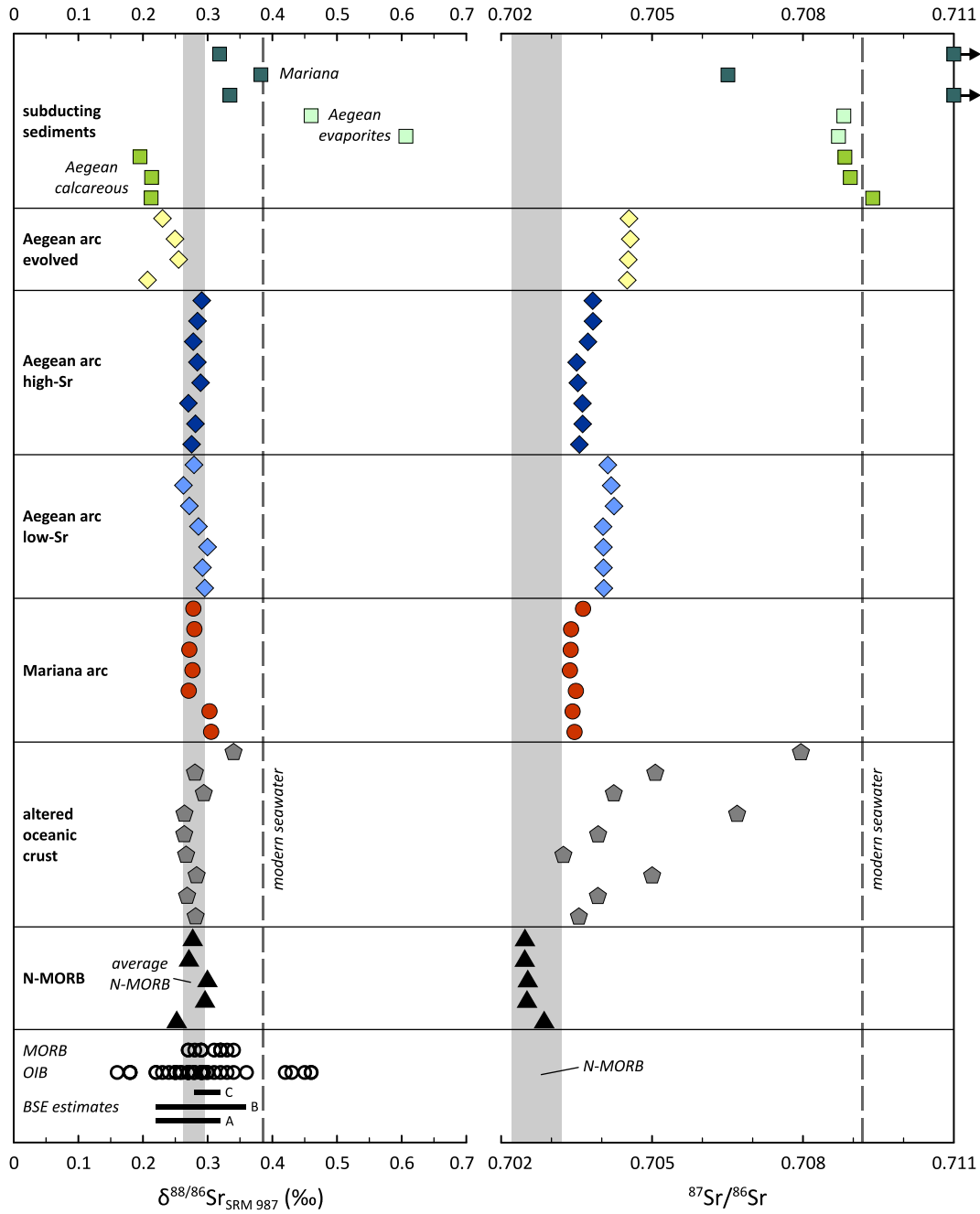
Figure 2. $\delta^{88/86}Sr$ and $^{87}Sr/^{86}Sr$ compositions of the studied samples; uncertainties are smaller than symbol size. Two Mariana sediment samples (pelagic clay and radiolarite-claystone) have $^{87}Sr/^{86}Sr$ of 0.7121 and 0.7181 and fall outside the scale of the figure. The grey bar for the $\delta^{88/86}Sr$ composition of N-MORB is the 95 % confidence interval of the N-MORB samples measured in this study. The composition of modern seawater is from McArthur et al. (2001) and Krabbenhöft et al. (2010) for $^{87}Sr/^{86}Sr$ and $\delta^{88/86}Sr$, respectively. Literature data for MORB and OIB $\delta^{88/86}Sr$ (open black triangles and circles, respectively) are shown for comparison (Moynier et al., 2010; Charlier et al., 2012; Andrews and Jacobson, 2017; Amsellem et al., 2018). Estimates of the $\delta^{88/86}Sr$ composition of the bulk silicate Earth (BSE) are from: A – Moynier et al. (2010), B – Charlier et al. (2012), C – Amsellem et al. (2018).

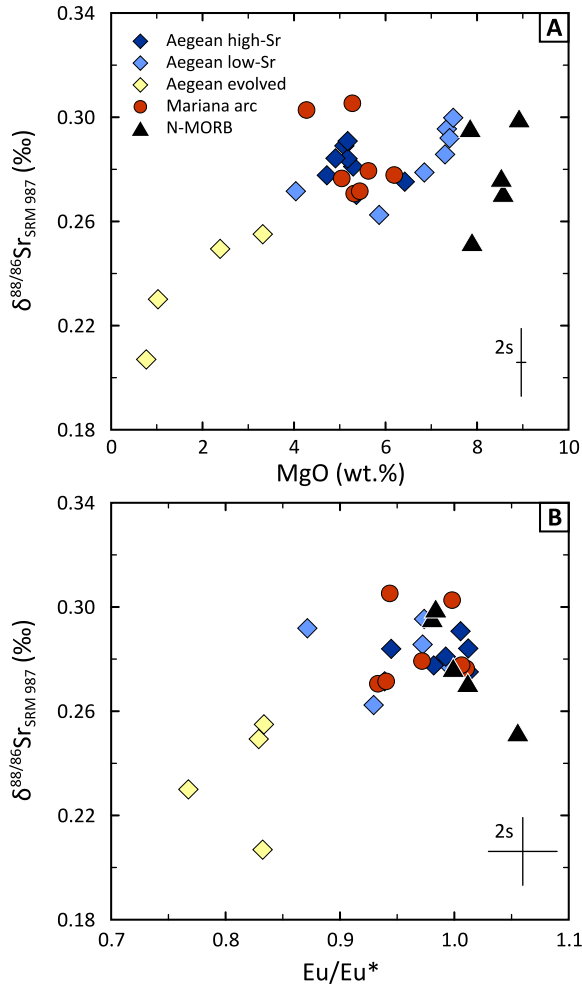**Figure 3.** Variation in $\delta^{88/86}Sr$ as a function of indices of the degree of magma differentiation: MgO content (a) and Eu/Eu* (b). The Eu anomaly (Eu/Eu*) is $Eu_N/(Sm_N \cdot Gd_N)^{1/2}$, where the subscript "N" denotes chondrite-normalised (McDonough and Sun, 1995) concentrations.

4. Discussion

4.1. Sr isotope fractionation during igneous differentiation

In order to assess the effects of fractional crystallisation on mass-dependent Sr systematics of our arc lavas, we measured several more evolved (andesite to rhyodacite) samples from the Aegean arc. For lavas with >4 wt.% MgO, we find no significant correlation between $\delta^{88/86}Sr$ and MgO content or Eu anomaly (Eu/Eu*; Figure 3). This is consistent with the lack of resolvable Sr isotope fractionation in the Kilauea Iki lava lake samples measured by Amsellem et al. (2018), which are related through the fractionation and accumulation of olivine and clinopyroxene (e.g., Helz, 2012). In contrast, the evolved Aegean arc samples have lower $\delta^{88/86}Sr$ that roughly correlates with degree of differentiation (Figure 3). An overall similar relationship between $\delta^{88/86}Sr$ and Eu/Eu* was found by Charlier et al. (2012). These authors attributed decreasing $\delta^{88/86}Sr$ predominantly to the fractionation of isotopically heavy plagioclase. The significant $\delta^{88/86}Sr$ heterogeneity in evolved samples in that study, however, requires modulation by other phases such as alkali-feldspar, biotite or amphibole in addition to plagioclase. Plagioclase is the main host of Sr in the Aegean arc lavas yet the lack of a clear correlation between $\delta^{88/86}Sr$ and Eu/Eu* suggests that amphibole crystallisation can also have an influence on Sr isotope fractionation. In addition, the higher $^{87}Sr/^{86}Sr$ of the evolved samples suggests minor crustal assimilation during magmatic differentiation, which could also contribute to the scatter in $\delta^{88/86}Sr$ of the evolved samples.

Most mafic Aegean and Mariana arc lavas have Eu/Eu* between 0.95 and 1.02, which suggests that the Sr isotope composition of these primitive lavas has not been affected by fractional crystallisation or accumulation of plagioclase. Two low-Sr Aegean and two Mariana arc samples with Eu/Eu* between 0.87 and 0.95 and lower Sr/Nd relative to other samples in their suite potentially show some evidence for the removal of plagioclase.

Their $\delta^{88/86}$Sr is on the lower end of the distribution yet not significantly different from the other samples. The identical average $\delta^{88/86}$Sr and similar Eu/Eu* of the Aegean low-Sr and high-Sr suites effectively rules out plagioclase removal or accumulation as the origin of the difference in Sr content and Sr/Nd between these two suites, which is consistent with major element and petrographic observations that do not support the presence of (resorbed) accumulated plagioclase in the high-Sr lavas. Hence, $\delta^{88/86}$Sr systematics of the samples in this study are not or only minimally modified by crustal processes and reflect the $\delta^{88/86}$Sr of the primary magmas delivered to the crustal magmatic systems in the Aegean and Mariana arcs.
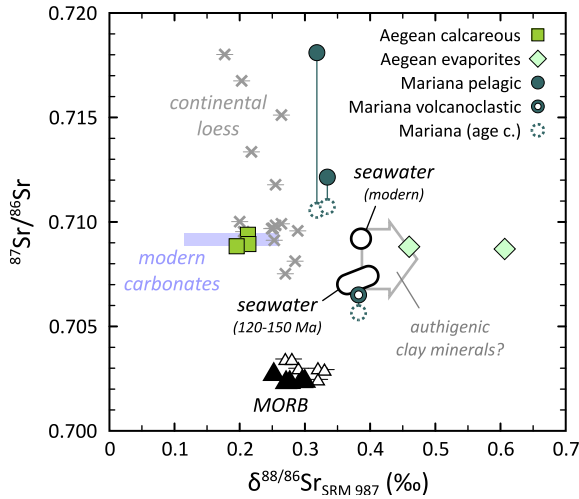

Figure 4. *Strontium isotope systematics of marine sediments from this study; where no error bars are shown, uncertainties are smaller than symbol size. Data for MORB (see Figure 2 for data sources), modern and 120-150 Ma seawater (McArthur et al., 2001; Krabbenhöft et al., 2010; Vollstaedt et al., 2014), continental loess (crosses; Pearce et al., 2015) and modern carbonates (Halicz et al., 2008; Krabbenhöft et al., 2010; Böhm et al., 2012; Vollstaedt et al., 2014) are shown for reference. Open circles for the Mariana sediments are age-corrected to their depositional age (Lancelot et al., 1990). The light grey arrow depicts the hypothetical composition of authigenic clay minerals that could form the high-$\delta^{88/86}$Sr component in the Mariana sediments; see text for discussion.*

4.2. The $\delta^{88/86}$Sr composition of subduction zone inputs

4.2.1. Mass-dependent Sr isotope systematics of marine sediments

Subducting sediments are a key component of arc magmas (e.g., White and Dupré, 1986; Plank and Langmuir, 1993) yet their $\delta^{88/86}$Sr composition is not well constrained. The Aegean and Mariana sediment samples measured in this study cover the most common Sr-rich lithologies of global marine sediments and thus contribute to the understanding of the composition of sedimentary Sr recycled into the mantle.

The calcareous Aegean sediments have uniform $\delta^{88/86}$Sr (0.195-0.213 ‰). As already indicated by their seawater-like ^{87}Sr/^{86}Sr composition, the Sr budget of the calcareous Aegean sediments is dominated by a marine carbonate component (Klaver et al., 2015). Previous studies have found that modern carbonates are isotopically light relative to seawater at $\delta^{88/86}$Sr = 0.17-0.21 ‰ (e.g., Halicz et al., 2008; Krabbenhöft et al., 2010; Böhm et al., 2012; Vollstaedt et al., 2014; Fruchter et al., 2017; Müller et al., 2018), with which calcareous Aegean sediments overlap (Figure 4). Although the Sr isotope fractionation factor between seawater and inorganic calcite is dependent on temperature and precipitation rate (Böhm et al., 2012; AlKhatib and Eisenhauer, 2017) and $\delta^{88/86}$Sr of seawater has been variable throughout the Phanerozoic, 0-500 Ma carbonates mostly have lower $\delta^{88/86}$Sr than MORB (Vollstaedt et al., 2014). This implies that the recycling of calcareous sediments into the mantle can remove isotopically light Sr from the oceans and form a low-$\delta^{88/86}$Sr component in the source of arc magmas.

In contrast, the three Mariana sediments are all isotopically heavy compared to MORB, and terrestrial igneous rocks in general, which requires an explanation (Figures 2 and 4). These sediments have been largely

deposited below the CCD, contain very little carbonate (Lancelot et al., 1990) and therefore lack the isotopically light Sr characteristic of the calcareous Aegean sediments. The general decrease in $\delta^{88/86}$Sr from mafic to felsic rocks (Figure 3) suggests that an andesitic bulk continental crust is likely to be isotopically light relative to MORB. We use the continental loess data of Pearce et al. (2015) as a proxy for continental detritus and the terrigenous component in the Pacific sediments. The loess samples are isotopically light and more radiogenic than MORB (Figure 4), consistent with our suggestion above about the composition of average continental crust. When ^{87}Sr/^{86}Sr is corrected to their depositional age, the pelagic Mariana sediments appear to lie on mixing lines between the loess data and a component with Cenozoic seawater-like ^{87}Sr/^{86}Sr (0.706-0.709) and $\delta^{88/86}$Sr that is similar to, or possibly slightly higher than, seawater (Figure 4). Similarly, the volcaniclastic turbidite sample, which is derived from a nearby mafic seamount chain (Lancelot et al., 1990), has higher $\delta^{88/86}$Sr and is more radiogenic than a mantle-derived component (represented by the MORB data in Figure 4). A possible explanation for the high $\delta^{88/86}$Sr of the Mariana sediments is that part of the Sr budget is hosted by authigenic clay minerals that have precipitated from seawater in a reverse weathering reaction. Such authigenic clay minerals have been shown to preferentially incorporate the heavier isotopes of Mg and thus have higher $\delta^{26/24}$Mg than seawater and the continental crust (Wimpenny et al., 2014; Dunlea et al., 2017). In case reverse weathering is associated with an isotopic fractionation of Sr in the same sense, authigenic clay minerals could constitute the component with $\delta^{88/86}$Sr similar or slightly higher than seawater in the Mariana sediments.

The two Messinian evaporite samples from the Eastern Mediterranean Sea display amongst the heaviest Sr isotope compositions found in natural rocks. Both have significantly higher $\delta^{88/86}$Sr yet similar ^{87}Sr/^{86}Sr to seawater, which is consistent with isotopic fractionation during precipitation, which enriches the solid phase in heavier isotopes. This is supported by an experimental study that found that anhydrite precipitation drove the composition of the liquid to isotopically lighter compositions, thus indicating that anhydrite has higher $\delta^{88/86}$Sr than liquid it precipitated from (Voigt et al., 2018). The extreme Sr isotope composition of the Messinian evaporites makes $\delta^{88/86}$Sr a potentially powerful tracer of the involvement of these evaporites in the source of the Aegean arc magmas.
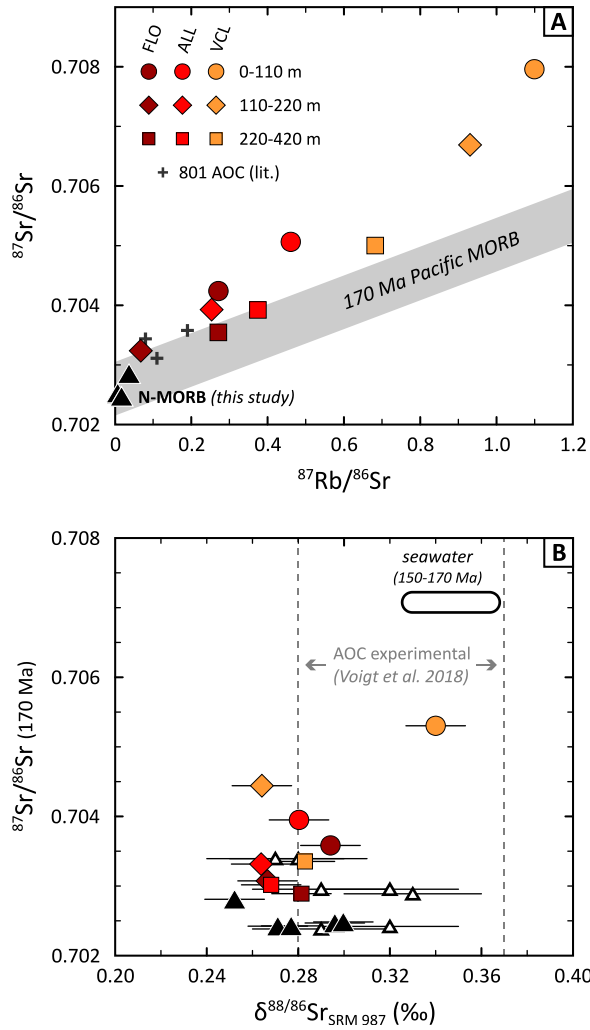
Figure 5. Strontium isotope systematics of altered oceanic crust (AOC) composite samples from ODP site 801 compared to the composition of fresh MORB. For each depth interval, three composite samples have been measured; the least altered (FLO) composites, most altered (VCL) composites and a weighted mean of all lithologies (ALL); a) $^{87}Rb/^{86}Sr$ versus $^{87}Sr/^{86}Sr$. The grey band shows the composition of modern Pacific MORB after 170 Ma radiogenic ingrowth. The black triangles are the N-MORB samples measured for $\delta^{88/86}Sr$ in this study; grey plusses are data for ODP 801 AOC from Hauff et al. (2003); b) age-corrected (to 170 Ma) $^{87}Sr/^{86}Sr$ versus $\delta^{88/86}Sr$. Only the 0-110 m VCL composite plots towards 170 Ma seawater (McArthur et al., 2001; Vollstaedt et al., 2014). The range in $\delta^{88/86}Sr$ of altered basalt from seawater reaction experiments (Voigt et al., 2018) is shown as dashed vertical lines as no radiogenic Sr data are reported for the reacted solid phases in that study. The composition of modern, unaltered MORB is shown as black triangles; filled symbols are from this study, open symbols are literature data (Charlier et al., 2012; Amsellem et al., 2018).

4.2.2. Mass-dependent Sr isotope systematics in (altered) oceanic crust

The $\delta^{88/86}Sr$ compositions of our N-MORB samples range from 0.252 to 0.300 ‰ with a mean of 0.279 ± 0.039 ‰. Indian MORB is isotopically lightest and Atlantic MORB heaviest, yet due to the limited number of measured MORB samples, these results cannot be used to make inferences about possible systematic variations between these ocean basins. Our data are in good agreement with other published means of MORB and ocean island basalts (0.27 ± 0.05 ‰ – Moynier et al., 2010; 0.29 ± 0.07 ‰ – Charlier et al., 2012; 0.276 ± 0.016 ‰ – Andrews and Jacobson, 2017; 0.30 ± 0.02 ‰ – Amsellem et al., 2018). The composition of N-MORB can be used to infer the $\delta^{88/86}Sr$ of the depleted MORB mantle. The lack of Sr isotope fractionation during fractional crystallisation of clinopyroxene in the Kilaeau Iki lava lake (Amsellem et al., 2018) suggests that the clinopyroxene-melt fractionation factor for Sr is small. As clinopyroxene hosts >90 % of the Sr budget in peridotites and Sr is incompatible during peridotite melting, it follows from an isotopic mass balance that the composition of N-MORB must closely approximate that of its mantle source. Support for this inference is provided by the overall identical average composition of MORB and ocean islands basalts (Moynier et al., 2010; Charlier et al., 2012; Andrews and Jacobson, 2017; Amsellem et al., 2018). As such, we can use the $\delta^{88/86}Sr$ composition of N-MORB to approximate that of the mantle wedge prior to any contamination with slab-derived components.

We present the first $\delta^{88/86}Sr$ data for the upper AOC through the measurement of composite samples from ODP site 801 in the western Pacific (Kelley et al., 2003). Although the use of composite samples invariably obscures part of the variation and underlying processes, composites are very useful in reducing potential sampling bias and to obtain a more reliable average composition for the AOC than can be derived from individual samples. The site 801 AOC composites have higher $^{87}Sr/^{86}Sr$ than modern unaltered Pacific MORB (Figure 5),

which is the combined result of radiogenic ingrowth and isotopic exchange with seawater (0.707-0.7092 for Jurassic to modern seawater; McArthur et al., 2001) during hydrothermal alteration at and near the ridge axis (e.g., Staudigel et al., 1995; Teagle et al., 1996). Figure 5a illustrates the effects of radiogenic ingrowth in the AOC composites. All AOC composites have elevated Rb/Sr compared to fresh MORB. The least altered AOC composites (110-420 m FLO and ALL) have age-corrected $^{87}Sr/^{86}Sr$ roughly within the range of 170 Ma Pacific MORB and hence their higher measured $^{87}Sr/^{86}Sr$ appears to be predominantly caused by radiogenic ingrowth at elevated Rb/Sr. This is supported by the relatively invariant Sr concentrations in these composites that are not significantly enriched compared to the Sr contents of fresh glasses (Kelley et al., 2003; see Table 1). A clear isotopic signature of Sr exchange with seawater, evident as an excess in $^{87}Sr/^{86}Sr$ compared to 170 Ma radiogenic ingrowth, is only observed in the three 0-110 m and the 110-220 m VCL AOC composites (Figure 5a). The range in age-corrected $^{87}Sr/^{86}Sr$ of the ODP site 801 upper crust is similar to that found for other drilled AOC sections such as site 417/418 in the Atlantic (0.7035-0.7062; Staudigel et al., 1995) and sites 504B, 896A (0.7025-0.7055; Teagle et al., 1998) and 1256D (0.7028-0.7061; Harris et al., 2015) in the eastern Pacific.

The AOC composites show remarkably little variation in $\delta^{88/86}Sr$ and only the most radiogenic 0-110 VCL composite sample has $\delta^{88/86}Sr$ that is significantly heavier than unaltered MORB; all other AOC composites overlap with our data for N-MORB (Figure 5b). The 0-110 m VCL composite sample plots towards the composition of 150-170 Ma seawater (McArthur et al., 2001; Vollstaedt et al., 2014) and has similar $\delta^{88/86}Sr$ to the basaltic material altered by seawater in the experimental study of Voigt et al. (2018). These authors found that alteration by seawater preferentially removes the lighter Sr isotopes from the basaltic host due to non-stoichiometric dissolution of crystalline basalt, but our results indicate that, at site 801, a positive shift in $\delta^{88/86}Sr$ is only observed in the most strongly altered fractions of the upper oceanic crust. Less altered composite samples can show a mild increase in age-corrected $^{87}Sr/^{86}Sr$ through exchange with seawater (e.g., 110-220 m VCL and 0-110 m ALL; Figure 5b) but without a discernible shift in $\delta^{88/86}Sr$.

4.3. A Sr isotope perspective on recycling in subduction zones

Radiogenic Sr isotope variations of arc lavas have long been a focus of attention for investigating the mechanisms of slab to mantle wedge mass transfer (e.g., Hawkesworth et al., 1977), commonly in combination with other radiogenic isotope systems such as $^{143}Nd/^{144}Nd$, which is a useful tracer of the proportion of subducted sediment in their source. Traditionally, Sr-Nd isotope variations have been interpreted to require two distinct slab-derived contributions, a sediment melt and a fluid derived from the altered oceanic crust (e.g., Elliott, 2003), but alternative interpretations have recently gained in popularity. Most notably, Nielsen and Marschall (2017) propose that Sr-Nd isotope systematics of global arc lavas are consistent with partial melting of a mélange, a physical mixture of bulk subducted sediments and the mantle wedge. The $\delta^{88/86}Sr$ systematics of arc lavas offer a new line of evidence that can be used to interrogate the different models for Sr recycling in subduction zones.
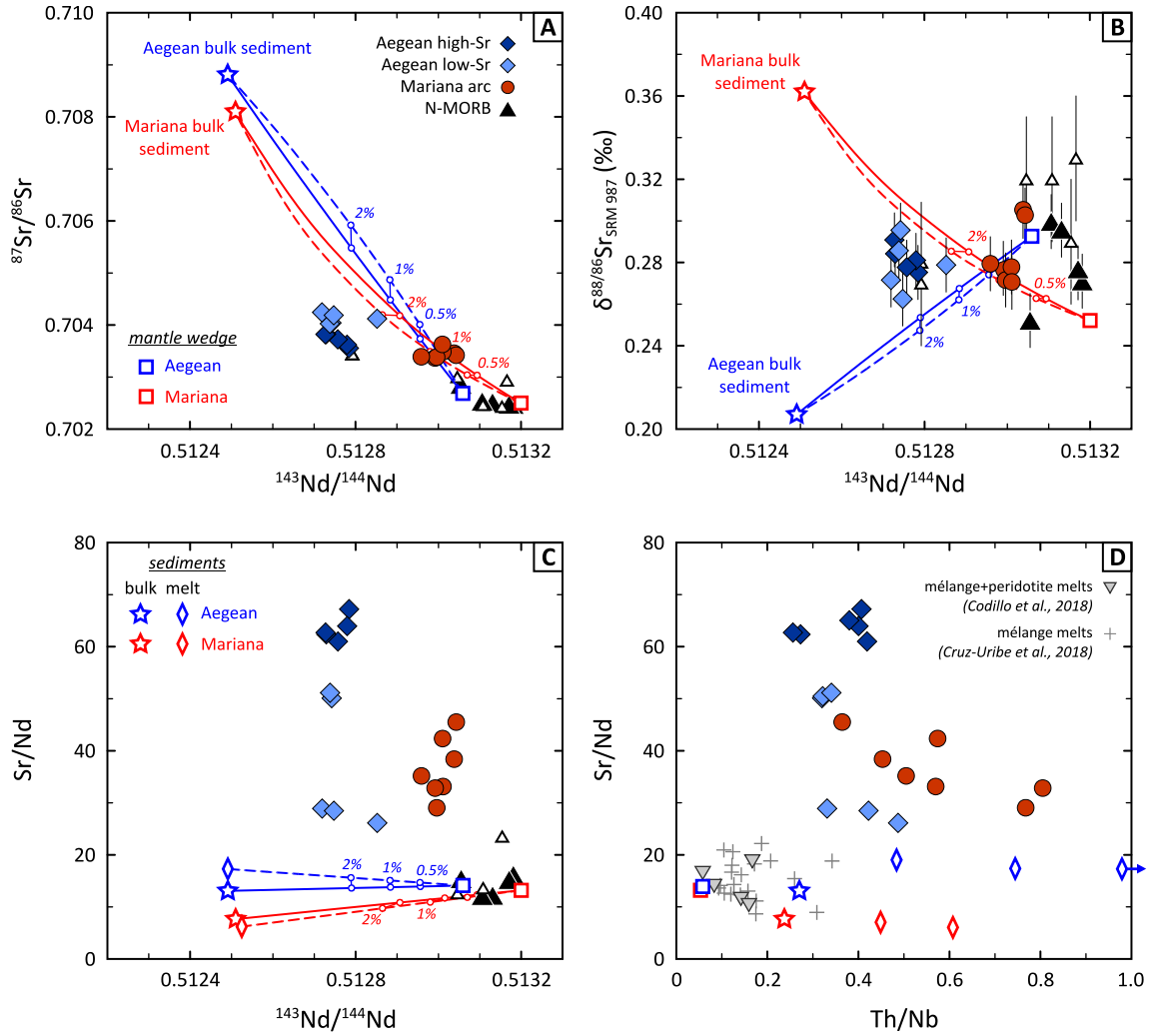
Figure 6. *The effect of sediment addition on $^{87}Sr/^{86}Sr$-$\delta^{88/86}Sr$-$^{143}Nd/^{144}Nd$ and trace element systematics of Aegean and Mariana arc lavas. MORB data (open triangles are literature data; see Figure 2) are shown for comparison; a) $^{143}Nd/^{144}Nd$ versus $^{87}Sr/^{86}Sr$; b) $^{143}Nd/^{144}Nd$ versus $\delta^{88/86}Sr$; c) $^{143}Nd/^{144}Nd$ versus Sr/Nd; d) Th/Nb versus Sr/Nd. Uncertainties on $^{143}Nd/^{144}Nd$ and $^{87}Sr/^{86}Sr$ are smaller than symbol size. The model curves show the effect of the addition of bulk sediment (solid lines) and partial melts thereof (dashed lines) to an appropriate mantle wedge composition. For the Aegean arc, the slightly enriched mantle wedge composition is taken from Klaver et al. (2016) and $\delta^{88/86}Sr$ is average Atlantic MORB from this study and Amsellem et al. (2018). For the Mariana arc the trace element composition of the mantle wedge is the depleted MORB mantle (Workman and Hart, 2005); $^{143}Nd/^{144}Nd$ and $^{87}Sr/^{86}Sr$ are that of the most primitive Mariana Trough sample (Gribble et al., 1996) and $\delta^{88/86}Sr$ is equivalent to the isotopically lightest reported value for MORB (the Indian MORB sample from this study). The average compositions of Mariana and Aegean arc sediments are from Plank and Langmuir (1998) and Klaver et al. (2015), respectively. The sediment partial melts are experimentally derived for appropriate starting materials for the Mariana (red diamonds; Martindale et al., 2013) and Aegean arc (blue diamonds; Skora et al., 2015); see text for discussion. In panel d), partial melts of natural mélange (Cruz-Uribe et al., 2018) and peridotite hybridised with mélange (Codillo et al., 2018) are shown. See supplementary Table S6 for the composition of the mixing components.*

4.3.1. Sediment addition alone does not account for Sr-Nd elemental and isotope systematics

Aegean lavas have amongst the lowest $^{143}Nd/^{144}Nd$ of global mafic island arc basalts, which reflects the significant role of recycled sediment in their petrogenesis (e.g., Bailey et al., 2009; Klaver et al., 2016; Elburg and Smet, 2020), whereas Mariana arc lavas display more radiogenic $^{143}Nd/^{144}Nd$ typical of island arc lavas. The Sr-Nd isotope data of the Aegean arc lavas are difficult to reconcile with bulk sediment addition. Figure 6a-c shows a

binary mixing relationship between a slightly enriched Aegean mantle wedge (Klaver et al., 2016) and bulk Aegean sediments (Klaver et al., 2015). The mismatch in $^{87}Sr/^{86}Sr$ with a binary mixing relationship is notable, but whether $\delta^{88/86}Sr$ is permissive of bulk sediment addition depends on the unknown $\delta^{88/86}Sr$ of the Aegean mantle wedge. In Figure 6, we have taken the average $\delta^{88/86}Sr$ of the six published Atlantic MORB samples (this work; Amsellem et al., 2018) as most representative. Sediment mixing with such a mantle wedge composition cannot explain the $\delta^{88/86}Sr$-$^{143}Nd/^{144}Nd$ composition of the Aegean lavas (Figure 6b). To obtain a decent fit with the Aegean lavas for $\delta^{88/86}Sr$, the Aegean mantle wedge needs to have an unusually heavy Sr isotope composition compared to published MORB values ($\delta^{88/86}Sr$ ~0.34 ‰), but even in this case the mismatch in $^{87}Sr/^{86}Sr$ remains robust. Taken together, Sr-Nd isotope systematics argue against bulk sediment addition and a mélange scenario in the Aegean arc. In case of the Mariana arc, a relatively large uncertainty on the $\delta^{88/86}Sr$ of the mantle wedge, in combination with a small amount of sediment addition, makes the constraints from Sr and Nd isotopes alone rather undiagnostic. Nonetheless, a mantle source consisting of depleted peridotite mixed with ~1 % bulk sediment (Plank and Langmuir, 1998) can reasonably account for the Sr-Nd isotope compositions of Mariana arc lavas only if the Mariana mantle wedge is ascribed the lowest measured $\delta^{88/86}Sr$ for MORB (Figure 6b).

Moreover, melting of a mélange that is a mixture of bulk sediment and mantle wedge cannot recreate key trace element ratios, notably Sr/Nd, in the Aegean and Mariana arc lavas (Figure 6c). The model of Nielsen and Marschall (2017) relies on Sr/Nd fractionation during partial melting of the mélange, aided by the retention of Nd by accessory phases. Subsequent experimental studies, however, did not bolster these predictions. Melting of natural mélange lithologies (Cruz-Uribe et al., 2018) or a mixture of mélange and peridotite (Codillo et al., 2018) does not fractionate Sr/Nd and hence fails to reproduce the significantly higher Sr/Nd of both Aegean and Mariana arc lavas relative to MORB and subducting sediments (Figure 6d). Furthermore, these experimental melts do not yield a notable negative Nb anomaly (which would be expressed as high Th/Nb in Figure 6d), one of the geochemical hallmarks of convergent margin magmas. Conceptually, this makes sense as the key accessory phases required to fractionate these trace elements (e.g., rutile and zoisite) are less likely to be present in the ultramafic environment of a mélange, where their key constituent elements (e.g., Ti, Al, Ca) are at lower abundances than in the subducting crust.

High Th/Nb of arc lavas is commonly attributed to residual rutile during partial melting of the upper oceanic crust and overlying sedimentary cover at sub-arc depths (e.g., Elliott et al., 1997). Adding the sedimentary component as a partial melt to the mantle wedge is, however, unlikely to alleviate the mismatch of the Aegean lavas with a bulk sediment-mantle wedge mixing model (figure 6a-b). To obtain a better fit in Sr-Nd isotope space, a sediment melt with lower Sr/Nd than bulk sediment would be required whereas the Aegean (and Mariana) lavas have markedly higher Sr/Nd (Figure 6c). The magnitude of Sr/Nd fractionation during sediment melting is contentious. Several experimental studies report low LREE contents and high Sr/Nd in sediment partial melts whereas others find very little fractionation of Sr/Nd. An explanation for this paradox is that certain experimental studies (e.g., Hermann and Rubatto, 2009; Skora and Blundy, 2010) might overestimate the magnitude of Sr/Nd fractionation during sediment melting. Doping of the experimental starting materials with LREE far in excess of natural concentrations enhances the stability of monazite, which strongly retains LREE. The presence of residual monazite in such doped experiments leads to erroneously high Sr/Nd in the melt phase (Skora and Blundy, 2012). Undoped experimental studies on appropriate sediment compositions reveal significantly less Sr/Nd fractionation. For instance, Skora et al. (2015) investigated trace element partitioning during melting of calcareous sediments that are very similar in $CaCO_3$ content and Sr/Nd to bulk Aegean sediments. These authors found that Sr/Nd of partial melts of such sediment compositions are only mildly elevated compared to bulk compositions (Figure 6c) as Sr is partially retained in residual carbonate up to high degrees of melting. The experimental study of Martindale et al. (2013) on volcaniclastic sediments subducting at the Mariana trench also found negligible Sr/Nd fractionation during melting although no clear repository for Sr could be identified in the residue.

Based on these lines of evidence, we argue that a two-component source or mélange, consisting of subducting sediments and mantle wedge, cannot account for the combined Sr-Nd systematics of the Mariana and Aegean arc lavas. While for many island arcs $^{87}Sr/^{86}Sr$-$^{143}Nd/^{144}Nd$ systematics are permissive of binary mixing with bulk sediment (Nielsen and Marschall, 2017), the MORB-like $\delta^{88/86}Sr$ precludes this in this case of the Aegean

arc lavas. Furthermore, high Sr/Nd in both the Aegean and Mariana arc lavas is clearly inconsistent with such a two-component source, regardless whether the sedimentary component is added in bulk or as a partial melt.
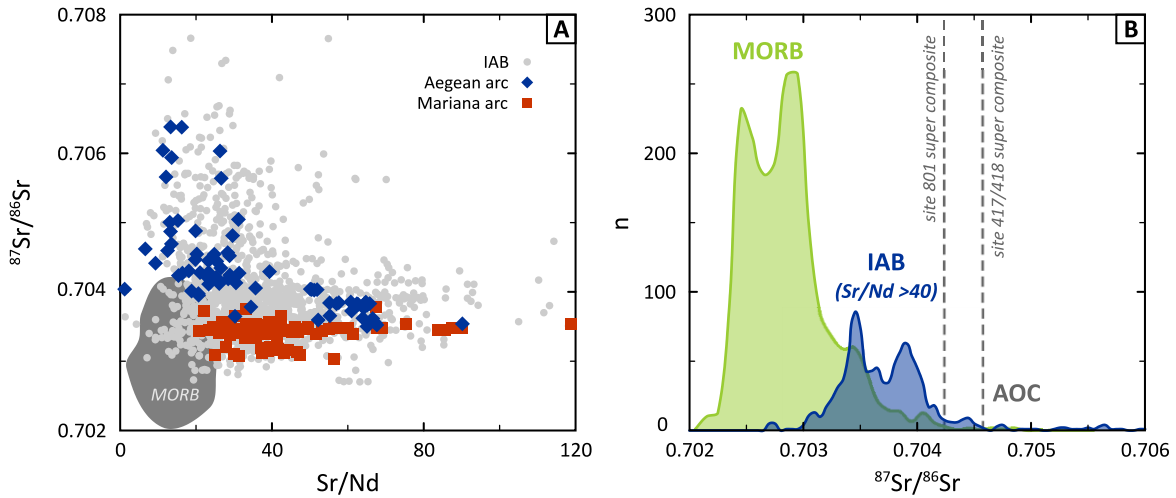

Figure 7. *Sr isotope systematics of global island arc basalts (IAB); a) Sr/Nd versus $^{87}Sr/^{86}Sr$ of global island arc basalts (<57 wt.% SiO_2; data compiled from GeoROC are provided in supplementary Dataset 2) with Aegean and Mariana arc samples highlighted. The variation in $^{87}Sr/^{86}Sr$ diminishes with increasing Sr/Nd, suggesting the presence of a global high-Sr/Nd component with $^{87}Sr/^{86}Sr$ ~0.7033-0.7042; b) histograms of $^{87}Sr/^{86}Sr$ in MORB and IAB with Sr/Nd >40, illustrating that $^{87}Sr/^{86}Sr$ in IAB is offset from MORB and AOC super composites for site 801 (this study) and 417/418 (Staudigel et al., 1995).*

4.3.2. Sr systematics of global island arc basalts

The Sr isotope mismatch in sediment-mantle wedge mixing models (Figure 6) calls for an additional component with a high Sr content, unradiogenic $^{87}Sr/^{86}Sr$ and MORB-like $\delta^{88/86}Sr$ in the source of arc magmas. As mentioned above, such a component has traditionally been considered to be an aqueous fluid derived from the altered mafic part of the slab and appears to be a common feature in global island arc basalts (IAB; see Elliott, 2003). In a compilation of global IAB data, Sr/Nd extends to higher values and is more variable in samples with unradiogenic $^{87}Sr/^{86}Sr$. This is more evident when individual arc suites are considered as these commonly display relatively invariable $^{87}Sr/^{86}Sr$ at Sr/Nd >40 (Figure 7; supplementary Figure S3). High Sr/Nd could be related to plagioclase accumulation in individual samples, but this can be confidently ruled out in the Aegean and Mariana samples based on petrography, major element evidence, Eu/Eu* near unity and constant $\delta^{88/86}Sr$. Conversely, arc lavas with $^{87}Sr/^{86}Sr$ >0.7045 and Sr/Nd <40 are likely to have been affected by fractional crystallisation of plagioclase accompanied by assimilation of crustal lithologies with radiogenic $^{87}Sr/^{86}Sr$. This is, for instance, illustrated by samples from the western side of the Aegean arc that have a strong crustal assimilation signature (Figure 7); note that the Aegean arc samples in this study derive from the eastern end of the Aegean arc, where the modification through assimilation is minimal (e.g., Elburg et al., 2014). Thus, the global signature of high and variable Sr/Nd at unradiogenic $^{87}Sr/^{86}Sr$ of IAB is unlikely to be caused by crustal processes and represents a feature of the primary magmas delivered to arc volcanic systems.

On a global scale, IAB converge to unradiogenic $^{87}Sr/^{86}Sr$ with 80 % of IAB with Sr/Nd >40 between 0.7033 and 0.7042 (median $^{87}Sr/^{86}Sr$ = 0.70366). As such, $^{87}Sr/^{86}Sr$ of global IAB is notably higher than MORB (Figure 7b) yet lower than the extrusive sections of altered oceanic crust (upper AOC). The latter generally has $^{87}Sr/^{86}Sr$ >0.7040 (this study; Staudigel et al., 1995), although for younger oceanic crust $^{87}Sr/^{86}Sr$ might be lower due to less radiogenic ingrowth (Teagle et al., 1998; Harris et al., 2015). The positive correlation between $^{87}Sr/^{86}Sr$ and H_2O content of AOC found by Staudigel et al. (1995) implies that most water is bound by the mafic crust that suffered the strongest alteration. Hence, dehydration of AOC should produce a fluid with a composition that is biased towards the more altered compositions, such as the VCL composites in this study and Staudigel et al.

(1995). Having such a fluid as a Sr-rich component in the source of arc magmas is not tenable from an $^{87}Sr/^{86}Sr$ viewpoint and also inconsistent with the high $\delta^{88/86}Sr$ of the most altered AOC composite (Figure 5) that is not recorded in either Aegean or Mariana arc lavas, potentially with the exception of the two Guguan samples ($\delta^{88/86}Sr$ ~0.305 ‰) from the Mariana arc.

The discrepancy between $^{87}Sr/^{86}Sr$ of arc suites, AOC and subducting sediments has also been noted by, for instance, Hawkesworth et al. (1993), Class et al. (2000) and Elliott (2003). Several explanations have been put forward, but most rely on specific local conditions such as the subduction of less altered mafic oceanic crust (e.g., Turner and Langmuir, 2015). Yogodzinski et al. (2017) propose that a partial melt of the deeper, unaltered oceanic crust is the source of the highly unradiogenic $^{87}Sr/^{86}Sr$ and high Sr contents of Aleutian arc lavas. Melting of the deeper sections of the slab is a possible explanation for specific locations where the subducting slab is unusually hot or where slab tears expose deeper portions of the oceanic crust but seems implausible as a global process. For instance, the Mariana and Tonga subduction zones are amongst the coldest globally (Syracuse et al., 2010) yet their arc lavas follow the global trend and range to high Sr/Nd at unradiogenic $^{87}Sr/^{86}Sr$. Thermal models suggest that while the topmost AOC might undergo fluid-induced partial melting, for which there is evidence from Th isotopes (Freymuth et al., 2016), the deeper parts of the oceanic crust do not normally reach their wet solidus temperature (van Keken et al., 2011). Instead, we propose that the missing component with an unradiogenic Sr isotope signature and high-Sr/Nd is a fluid that acquired its distinct geochemical signature in the less altered lower oceanic crust and sheeted dyke complex.
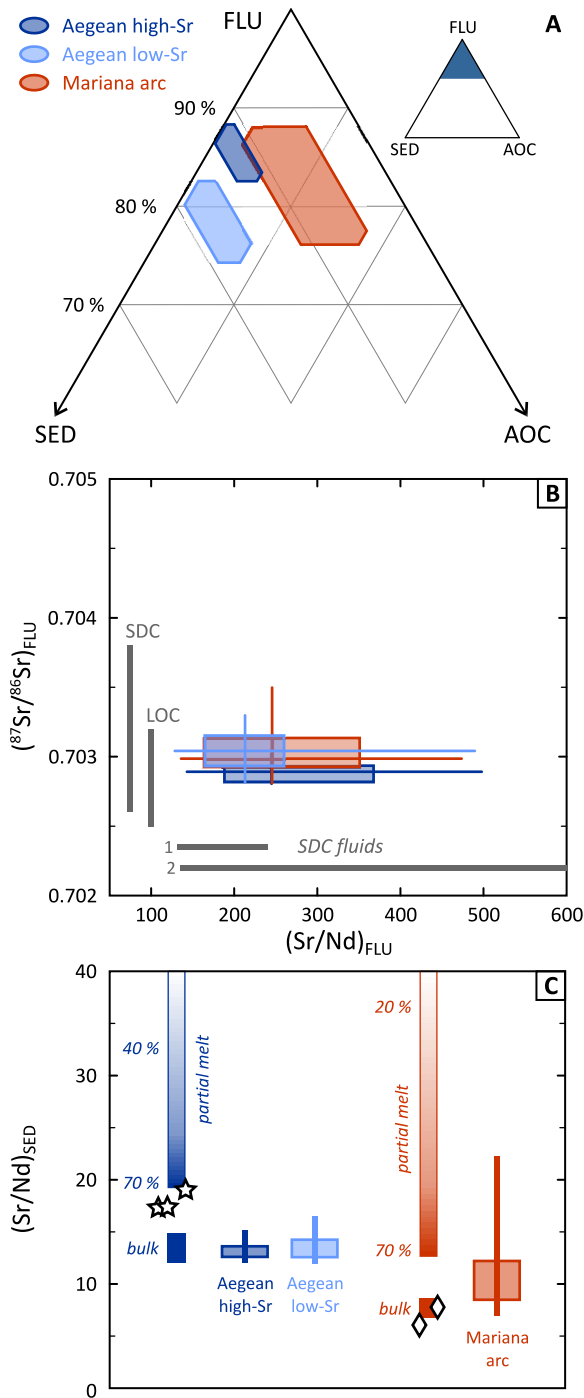
Figure 8. Results of inverse Sr-Nd modelling for the Aegean and Mariana arc lavas. See text and Table 2 for details on the modelling approach; a) ternary diagram showing the relative contributions of the three slab components (sediment – SED, altered oceanic crust – AOC and serpentinite-derived slab fluid – FLU) to the Sr budget of the arc lavas, projected from the depleted mantle wedge (DMM) component. More than 70 % of Sr is contributed by the fluid phase, even for the Aegean arc lavas that carry a strong sediment signature; b) box-and-whisker diagram showing the model composition of the serpentinite-derived slab fluid (FLU). The slab fluid has an $^{87}Sr/^{86}Sr$ signature that overlaps with the $^{87}Sr/^{86}Sr$ of the lower oceanic crust (LOC; e.g., Lécuyer and Gruau, 1996; Bach et al., 2001) and the sheeted dyke complex (SDC; e.g., Teagle et al., 1998; Harris et al., 2015). Sr/Nd of the slab fluid is less well constrained but is found to be >100, consistent with fluids in equilibrium with the sheeted dyke complex using the fluid-eclogite partition coefficients of Kessel et al. (2005) and Rustioni et al. (2019) (SDC fluid 1 and 2, respectively); c) box-and-whisker diagram showing the Sr/Nd of the sediment component (SED) in comparison to the bulk composition of Aegean and Mariana sediments (Plank and Langmuir, 1998; Klaver et al., 2015) and partial melts thereof using partition coefficients from Hermann and Rubatto (2009). The symbols show Sr/Nd of experimental sediment melts performed on appropriate (undoped) bulk sediment compositions at >800 °C. Stars are experiments on calcareous sediments with bulk Sr/Nd identical to the Aegean sediments (Skora et al., 2015); diamonds are experimental melts of Mariana volcaniclastic sediments (Martindale et al., 2013).

4.3.3. The important role of serpentinite-derived fluids

It is increasingly recognised that the breakdown of serpentinite may be the main source of fluid delivered to the mantle wedge at sub-arc depths (e.g., Ringwood, 1974; John et al., 2004; Scambelluri et al., 2004; Spandler and Pirard, 2013; Cooper et al., 2020). The upper mantle section of the slab can be hydrated when the plate bends and faults near the trench (e.g., Ranero et al., 2003; Van Avendonk et al., 2011) and has been argued to form a major carrier of water into the mantle (Cai et al., 2018), although the effectiveness of serpentinization at the trench has been challenged by Korenaga (2017). Whereas dehydration of the AOC and sedimentary package is continuous but mostly achieved in the forearc region (Schmidt and Poli, 1998; van Keken et al., 2011), serpentinite is stable to higher pressure and has the potential to release significant quantities of water at sub-arc depths mainly through the breakdown of antigorite (Ulmer and Trommsdorff, 1999; Rüpke et al., 2004; Savage, 2012). Fluids generated by serpentinite breakdown in the slab migrate upwards through the overlying

16

oceanic crust, perhaps in short-lived and strongly channelised events (John et al., 2012; Plümper et al., 2017; Taetz et al., 2018) that have the potential to strip significant quantities of fluid mobile elements from the oceanic crust (Zack and John, 2007; Freymuth et al., 2015; Chen et al., 2019; Freymuth et al., 2019). As Sr is highly incompatible in an eclogite mineral assemblage (Kessel et al., 2005; Rustioni et al., 2019), fluids can liberate significant quantities of Sr from the mafic crust. In such a scenario, the original Sr isotope signature of serpentinite dehydration fluids, likely similar to seawater, will be overprinted by the Sr isotope composition of the oceanic crust through continuous isotopic exchange. Migrating up a temperature gradient, the infiltration of these external fluids can induce wet partial melting of the AOC, sediments and mantle wedge and as such form the medium through which a composite slab component is delivered to the source of arc magmas (Spandler and Pirard, 2013; Walowski et al., 2015; Freymuth et al., 2016).

In order to investigate whether a slab-derived fluid is the missing component to explain the $^{87}Sr/^{86}Sr$ and $\delta^{88/86}Sr$ systematics of arc lavas, we performed forward modelling of a set of Sr-Nd isotope and elemental mass balance equations for the mixing of four components: i) depleted MORB mantle (DMM), ii) subducted sediments, iii) AOC and iv) a fluid component. The actual Sr and Nd concentrations of the components are unimportant in this model as we employ the fraction of Sr derived from each component as the mixing parameter in conventional isotopic and elemental mass balance equations (see supplementary material for these equations). The model employs a Monte Carlo approach to determine which relative proportions of these components can reproduce the $^{87}Sr/^{86}Sr$, $\delta^{88/86}Sr$, $^{143}Nd/^{144}Nd$ and Sr/Nd compositions of the arc lava suites. Rather than adopting a fixed composition for each component, several parameters were allowed to vary independently (see supplementary Table S7). Principally, the composition of the fluid ($^{87}Sr/^{86}Sr$ and $\delta^{88/86}Sr$) is not known a priori and one aim of the modelling approach was to better constrain the nature of this component. In addition, Sr/Nd of the AOC and sediment component were permitted to vary from their bulk composition to higher values as some experimental studies report for AOC and sediment partial melts (e.g., Hermann and Rubatto, 2009; Skora and Blundy, 2010). More details on the inverse modelling approach are given in the online supplementary material and the results are summarised in Table 2 and Figure 8.

The modelling results indicate that an appropriate fluid component has unradiogenic $^{87}Sr/^{86}Sr$ (0.7028-0.7032) and MORB-like $\delta^{88/86}Sr$ (0.27-0.30 ‰) for both the Aegean and Mariana arc suites. Its Sr/Nd is poorly constrained at values >100 (Figure 8). The composition of this fluid phase matches that of a fluid in equilibrium with the lower oceanic crust and sheeted dyke complex (Figure 8). These sections of the oceanic crust have suffered less pervasive seawater alteration than the altered upper oceanic crust, which is expressed in $^{87}Sr/^{86}Sr$ that is only slightly to moderately elevated compared to fresh MORB glasses (e.g., Lécuyer and Gruau, 1996; Teagle et al., 1998; Bach et al., 2001; Harris et al., 2015). Although there are no direct constraints on the $\delta^{88/86}Sr$ composition of the lower oceanic crust, the lack of notable Sr isotope fractionation in most AOC composites (Figure 5) suggests that MORB-aqueous fluid interactions at high temperature are unlikely to perturb $\delta^{88/86}Sr$ from their original MORB-like values. Support for this assertion is provided by the MORB-like $\delta^{88/86}Sr$ composition of mid-ocean ridge hydrothermal fluids (Krabbenhöft et al., 2010; Pearce et al., 2015). As such, a fluid sourced from antigorite breakdown in the slab mantle that was transported through and equilibrated with the lower oceanic crust and sheeted dyke complex, is a viable candidate to be the high Sr/Nd component in Aegean and Mariana arc magmas.
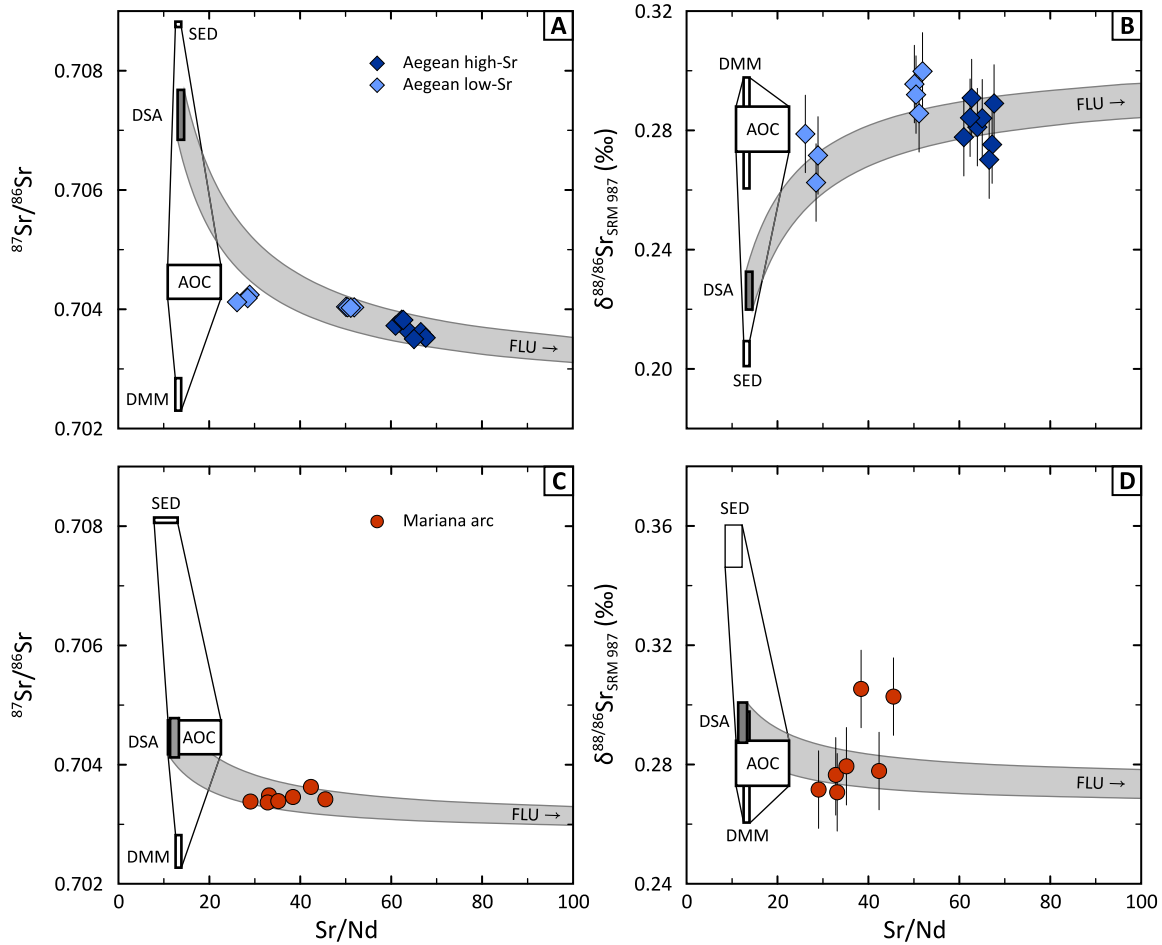
Figure 9. *Variation in $^{87}Sr/^{86}Sr$ and $\delta^{88/86}Sr$ as a function of Sr/Nd for the Aegean and Mariana arc lavas. The composition of the four components (depleted MORB mantle – DMM, subducted sediments – SED, altered oceanic crust – AOC and slab-derived fluid – FLU) are taken from the inverse modelling (see Table 2, Figure 8 and text for discussion). To illustrate mixing between the four components in a binary diagram, a mixing line between the fluid component and a combined DMM-Sediment-AOC (DSA; dark grey box) component is shown. This does not imply that we envisage addition of a fluid to a mélange-like mantle source but serves to illustrate that a variable fluid proportion can explain the difference between the Aegean low-Sr and high-Sr suites whereas the relative proportions of DMM-, sediment- and AOC-derived Sr are constant. The Aegean samples with the lowest Sr/Nd, however, require a smaller proportion of sediment-derived Sr in their source and/or a decrease of Sr/Nd through magmatic processes. For the Mariana arc, the two Guguan samples have significantly higher $\delta^{88/86}Sr$ and appear to require a slab-derived fluid with slightly higher $\delta^{88/86}Sr$.*

4.3.4. The Sr budget of arc magmas and implications for slab-wedge interaction

The inverse modelling results give an insight in how the Sr budget of the Aegean and Mariana arc lavas is composed (Figure 8). On average, 70-85 % of the total Sr budget of these arc lavas is derived from the fluid component that we infer has equilibrated with the less altered oceanic crust (Table 2). Strikingly, this applies to both the Mariana arc, which is traditionally regarded as a fluid-dominated arc based on trace element systematics (Figure 1), and the Aegean arc that has a much stronger sediment signature. The Aegean arc is unique in that 3-6 km of calcareous sediments are subducted, yet a carbonate Sr isotope signature is barely detectable as its contribution is overwhelmed by Sr contributed by the slab-derived fluid. Turner and Langmuir (2015) also suggested that subducted sediments have little leverage on the Sr budget of global arc lavas but attributed this to a large contribution of Sr from the AOC rather than a slab fluid from the deeper oceanic crust.

A second notable result is that Sr/Nd of the sediment component cannot be strongly fractionated from bulk sediment values (Figure 8). Higher sediment Sr/Nd values were found not to yield any permissible results, in

particular in the case of the Aegean arc lavas. As sediment melting seems to be required to generate the characteristic high Th/Nb of the Mariana and Aegean arc lavas (Figure 6), this result argues for limited Sr/Nd fractionation during sediment melting. The latter is in line with the experimental studies on compositions similar to bulk Aegean and Mariana sediments (Martindale et al., 2013; Skora et al., 2015) and tentatively suggests that anomalous LREE-retention in REE-doped starting materials (Hermann and Rubatto, 2009; Skora and Blundy, 2010, 2012) is indeed not representative of actual sediment melting at arcs.

Foremost, the Sr isotope constraints presented here highlight the crucial role of fluids released by the breakdown of serpentinite in arc magma genesis. Our preferred interpretation of the results is that the recycled component in the source of arc magmas is a wet partial melt of the AOC and sedimentary cover, where melting is induced by the arrival of a pulse of fluid derived from the lithospheric mantle of the subducting plate. The extent to which the AOC and sediments melt is dependent on the thermal parameters at the top of the slab and can vary from arc to arc. This model works well to explain the relatively constant $^{87}Sr/^{86}Sr$ and MORB-like $\delta^{88/86}Sr$ at variable Sr/Nd of the studied Aegean and Mariana arc lavas (Figure 9) and potentially global IAB. Aegean high-Sr and some low-Sr samples can be related through different proportions of fluid-derived Sr alone; the relative proportions of Sr derived from the DMM, sediments and AOC in these lavas are constant. A few low-Sr samples require additional variation in the proportion of sediment-derived Sr, and in the Mariana arc the two Guguan samples seem to require a distinct fluid $\delta^{88/86}Sr$ composition compared to the other lavas (Figure 9). Nevertheless, combined $^{87}Sr/^{86}Sr–\delta^{88/86}Sr$ systematics of arc lavas reveal that fluids derived from the deeper, less altered sections of the subducted oceanic crust are the dominant contributor to the Sr budget of arc magmas and can modulate their Sr isotopic composition on a global scale. Given their important role in controlling Sr systematics, such fluids are also expected to exert strong leverage on the budget of other elements that can be easily mobilised from the oceanic crust, such as for instance Pb, Mo and W (e.g., Miller et al., 1994; Freymuth et al., 2015; König et al., 2016; Mazza et al., 2020).

5. Conclusions

We have measured a suite of mafic volcanic rocks from the Aegean and Mariana arcs for their combined $^{87}Sr/^{86}Sr-\delta^{88/86}Sr$ systematics. The composition of these arc lavas is compared to N-MORB, altered oceanic crust composites and subducting sediments. The results of this study can be summarised as follows:

-   Mafic arc lavas have $\delta^{88/86}Sr$ identical to N-MORB and moderately altered oceanic crust; more evolved arc lavas trend towards isotopically lighter compositions.
-   Subducting sediments have highly variable $\delta^{88/86}Sr$; carbonate-rich sediments are homogeneous and isotopically lighter than MORB whereas carbonate-free sediments have $\delta^{88/86}Sr$ higher than MORB, potentially because part of the Sr budget is hosted in isotopically heavy authigenic clay minerals.
-   Sr-Nd isotope and elemental systematics indicate that the source of the Aegean and Mariana arc lavas cannot be a binary mixture between mantle wedge peridotite and bulk sediment (mélange). Partial melting of a mélange or sediment does not increase Sr/Nd to the values recorded in arc lavas; a fluid is required to fractionate Sr/Nd.
-   The combined $^{87}Sr/^{86}Sr-\delta^{88/86}Sr$ signature of mafic arc lavas indicates that >70 % of their Sr budget is contributed by a slab-derived fluid. This fluid is likely generated by the breakdown of serpentinite in mantle section of the subducting slab and subsequently migrates through and equilibrates with the overlying oceanic crust. The unradiogenic $^{87}Sr/^{86}Sr$ and MORB-like $\delta^{88/86}Sr$ of the fluid component indicates that it was last in equilibrium with the less-altered lower oceanic crust and sheeted dyke complex.
-   The Sr-Nd isotope composition of Aegean and Mariana arc lavas is best explained if the slab-derived fluid induces wet partial melting of the upper altered oceanic crust and sedimentary cover, which is then added as a composite metasomatic component to the mantle source of arc magmas.

- Even in the case of the Aegean arc where up to 6 km of Sr-rich calcareous sediments are subducted, the slab-derived fluid dominates the Sr budget and the sediments exert little control on the Sr isotope composition of the arc magmas.

Acknowledgements

References

AlKhatib, M. and Eisenhauer, A. (2017) Calcium and strontium isotope fractionation in aqueous solutions as a function of temperature and reaction rate; I. Calcite. *Geochim. Cosmochim. Acta* **209**, 296-319.

Amsellem, E., Moynier, F., Day, J.M., Moreira, M., Puchtel, I.S. and Teng, F.-Z. (2018) The stable strontium isotopic composition of ocean island basalts, mid-ocean ridge basalts, and komatiites. *Chem. Geol.* **483**, 595-602.

Andrews, M.G. and Jacobson, A.D. (2017) The radiogenic and stable Sr isotope geochemistry of basalt weathering in Iceland: role of hydrothermal calcite and implications for long-term climate regulation. *Geochim. Cosmochim. Acta* **215**, 247-262.

Avanzinelli, R., Prytulak, J., Skora, S., Heumann, A., Koetsier, G. and Elliott, T. (2012) Combined ^{238}U–^{230}Th and ^{235}U–^{231}Pa constraints on the transport of slab-derived material beneath the Mariana Islands. *Geochim. Cosmochim. Acta* **92**, 308-328.

Bach, W., Alt, J.C., Niu, Y., Humphris, S.E., Erzinger, J. and Dick, H.J. (2001) The geochemical consequences of late-stage low-grade alteration of lower ocean crust at the SW Indian Ridge: Results from ODP Hole 735B (Leg 176). *Geochim. Cosmochim. Acta* **65**, 3267-3287.

Bailey, J.C., Jensen, E., Hansen, A., Kann, A. and Kann, K. (2009) Formation of heterogeneous magmatic series beneath North Santorini, South Aegean island arc. *Lithos* **110**, 20-36.

Böhm, F., Eisenhauer, A., Tang, J., Dietzel, M., Krabbenhöft, A., Kisakürek, B. and Horn, C. (2012) Strontium isotope fractionation of planktic foraminifera and inorganic calcite. *Geochim. Cosmochim. Acta* **93**, 300-314.

Cai, C., Wiens, D.A., Shen, W. and Eimer, M. (2018) Water input into the Mariana subduction zone estimated from ocean-bottom seismic data. *Nature* **563**, 389.

Charlier, B.L.A., Nowell, G.M., Parkinson, I.J., Kelley, S.P., Pearson, D.G. and Burton, K.W. (2012) High temperature strontium stable isotope behaviour in the early solar system and planetary bodies. *Earth Planet. Sci. Lett.* **329**, 31-40.

Charlier, B.L.A., Parkinson, I.J., Burton, K.W., Grady, M.M., Wilson, C.J.N. and Smith, E.G.C. (2017) Stable strontium isotopic heterogeneity in the solar system from double-spike data. *Geochemical perspectives letters.* **4**, 35-40.

Chen, S., Hin, R.C., John, T., Brooker, R., Bryan, B., Niu, Y. and Elliott, T. (2019) Molybdenum systematics of subducted crust record reactive fluid flow from underlying slab serpentine dehydration. *Nature communications* **10**, 1-9.

Class, C., Miller, D.M., Goldstein, S.L. and Langmuir, C.H. (2000) Distinguishing melt and fluid subduction components in Umnak Volcanics, Aleutian Arc. *Geochem. Geophys. Geosyst.* **1**.

Clift, P. and Vannucchi, P. (2004) Controls on tectonic accretion versus erosion in subduction zones: Implications for the origin and recycling of the continental crust. *Rev. Geophys.* **42**.

Codillo, E., Le Roux, V. and Marschall, H. (2018) Arc-like magmas generated by mélange-peridotite interaction in the mantle wedge. *Nature communications* **9**, 1-11.

Cooper, G.F., Macpherson, C.G., Blundy, J.D., Maunder, B., Allen, R.W., Goes, S., Collier, J.S., Bie, L., Harmon, N. and Hicks, S.P. (2020) Variable water input controls evolution of the Lesser Antilles volcanic arc. *Nature* **582**, 525-529.

Coplen, T.B. (2011) Guidelines and recommended terms for expression of stable-isotope-ratio and gas-ratio measurement results. *Rapid communications in mass spectrometry* **25**, 2538-2560.

Cruz-Uribe, A.M., Marschall, H.R., Gaetani, G.A. and Le Roux, V. (2018) Generation of alkaline magmas in subduction zones by partial melting of mélange diapirs—An experimental study. *Geology* **46**, 343-346.

Dunlea, A.G., Murray, R.W., Ramos, D.P.S. and Higgins, J.A. (2017) Cenozoic global cooling and increased seawater Mg/Ca via reduced reverse weathering. *Nature communications* **8**, 1-7.

Elburg, M.A. and Smet, I. (2020) Geochemistry of lavas from Aegina and Poros (Aegean Arc, Greece): Distinguishing upper crustal contamination and source contamination in the Saronic Gulf area. *Lithos* **358-359**, 105416.

Elburg, M.A., Smet, I. and De Pelsmaeker, E. (2014) Influence of source materials and fractionating assemblage on magmatism along the Aegean Arc, and implications for crustal growth. *Geological Society, London, Special Publications* **385**, 137-160.

Elburg, M., Smet, I., Vanhaecke, F., Klaver, M. and Andersen, T. (2018) Extreme isotopic variation documents extensional tectonics in arc magmas from Methana, Greece. *Lithos* **318**, 386-398.

Elliott, T. (2003) Tracers of the slab, in: Eiler, J. (Ed.), *Inside the subduction factory*. American Gephysical Union, pp. 23-45.

Elliott, T., Plank, T., Zindler, A., White, W. and Bourdon, B. (1997) Element transport from slab to volcanic front at the Mariana arc. *Journal of Geophysical Research: Solid Earth* **102**, 14991-15019.

Francalanci, L., Varekamp, J., Vougioukalakis, G., Delant, M., Innocenti, F. and Manetti, P. (1995) Crystal retention, fractionation and crustal assimilation in a convecting magma chamber, Nisyros Volcano, Greece. *Bull. Volcanol.* **56**, 601-620.

Freymuth, H., Vils, F., Willbold, M., Taylor, R.N. and Elliott, T. (2015) Molybdenum mobility and isotopic fractionation during subduction at the Mariana arc. *Earth Planet. Sci. Lett.* **432**, 176-186.

Freymuth, H., Ivko, B., Gill, J.B., Tamura, Y. and Elliott, T. (2016) Thorium isotope evidence for melting of the mafic oceanic crust beneath the Izu arc. *Geochim. Cosmochim. Acta* **186**, 49-70.

Freymuth, H., Andersen, M.B. and Elliott, T. (2019) Uranium isotope fractionation during slab dehydration beneath the Izu arc. *Earth Planet. Sci. Lett.* **522**, 244-254.

Fruchter, N., Lazar, B., Nishri, A., Almogi-Labin, A., Eisenhauer, A., Shlevin, Y.B.e. and Stein, M. (2017) $^{88}Sr/^{86}Sr$ fractionation and calcite accumulation rate in the Sea of Galilee. *Geochim. Cosmochim. Acta* **215**, 17-32.

Gill, J. and Condomines, M. (1992) Short-lived radioactivity and magma genesis. *Science* **257**, 1368-1376.

Gribble, R.F., Stern, R.J., Bloomer, S.H., Stüben, D., O'Hearn, T. and Newman, S. (1996) MORB mantle and subduction components interact to generate basalts in the southern Mariana Trough back-arc basin. *Geochim. Cosmochim. Acta* **60**, 2153-2166.

Halicz, L., Segal, I., Fruchter, N., Stein, M. and Lazar, B. (2008) Strontium stable isotopes fractionate in the soil environments? *Earth Planet. Sci. Lett.* **272**, 406-411.

Harris, M., Coggon, R.M., Smith-Duque, C.E., Cooper, M.J., Milton, J.A. and Teagle, D.A. (2015) Channelling of hydrothermal fluids during the accretion and evolution of the upper oceanic crust: Sr isotope evidence from ODP Hole 1256D. *Earth Planet. Sci. Lett.* **416**, 56-66.

Hauff, F., Hoernle, K. and Schmidt, A. (2003) Sr-Nd-Pb composition of Mesozoic Pacific oceanic crust (Site 1149 and 801, ODP Leg 185): Implications for alteration of ocean crust and the input into the Izu-Bonin-Mariana subduction system. *Geochem. Geophys. Geosyst.* **4**.

Hawkesworth, C.J., O'Nions, R.K., Pankhurst, R.J., Hamilton, P.J. and Evensen, N.M. (1977) A geochemical study of island-arc and back-arc tholeiites from the Scotia Sea. *Earth Planet. Sci. Lett.* **36**, 253-262.

Hawkesworth, C., Gallagher, K., Hergt, J. and McDermott, F. (1993) Mantle and slab contributions in arc magmas. *Annual Review of Earth and Planetary Sciences* **21**, 175-204.

Helz, R.T. (2012) Trace-element analyses of core samples from the 1967-1988 drillings of Kilauea Iki lava lake, Hawaii, U.S. Geological Survey Open-File Report, p. 46.

Hermann, J. and Rubatto, D. (2009) Accessory phase control on the trace element signature of sediment melts in subduction zones. *Chem. Geol.* **265**, 512-526.

Horwitz, E.P., Chiarizia, R. and Dietz, M.L. (1992) A novel strontium-selective extraction chromatographic resin. *Solvent extraction and ion exchange* **10**, 313-336.

Ishikawa, T. and Nakamura, E. (1994) Origin of the slab component in arc lavas from across-arc variation of B and Pb isotopes. *Nature* **370**, 205-208.

John, T., Scherer, E.E., Haase, K. and Schenk, V. (2004) Trace element fractionation during fluid-induced eclogitization in a subducting slab: trace element and Lu–Hf–Sm–Nd isotope systematics. *Earth Planet. Sci. Lett.* **227**, 441-456.

John, T., Gussone, N., Podladchikov, Y.Y., Bebout, G.E., Dohmen, R., Halama, R., Klemd, R., Magna, T. and Seitz, H.-M. (2012) Volcanic arcs fed by rapid pulsed fluid flow through subducting slabs. *Nat. Geosci.* **5**, 489-492.

Karl, S.M., Wandless, G.A. and Karpoff, A.-M. (1992) Sedimentological and geochemical characteristics of leg 129 siliceous deposits, *Proceedings of the Ocean Drilling Program, Scientific Results*, College Station, TX.

Karpoff, A.-M. (1992) Cenozoic and Mesozoic sediments from the Pigafetta bason, leg 129, sites 800 and 801: Mineralogical and geochemical trends of the deposits overlying the oldest oceanic crust, *Proceedings of the Ocean Drilling Program, Scientific Results*, College Station, TX.

Kelley, K.A., Plank, T., Ludden, J. and Staudigel, H. (2003) Composition of altered oceanic crust at ODP Sites 801 and 1149. *Geochem. Geophys. Geosyst.* **4**.

Kessel, R., Schmidt, M.W., Ulmer, P. and Pettke, T. (2005) Trace element signature of subduction-zone fluids, melts and supercritical liquids at 120–180 km depth. *Nature* **437**, 724-727.

Klaver, M., Djuly, T., de Graaf, S., Sakes, A., Wijbrans, J., Davies, G. and Vroon, P. (2015) Temporal and spatial variations in provenance of Eastern Mediterranean Sea sediments: Implications for Aegean and Aeolian arc volcanism. *Geochim. Cosmochim. Acta* **153**, 149-168.

Klaver, M., Davies, G.R. and Vroon, P.Z. (2016) Subslab mantle of African provenance infiltrating the Aegean mantle wedge. *Geology* **44**, 367-370.

Klaver, M., Blundy, J.D. and Vroon, P.Z. (2018) Generation of arc rhyodacites through cumulate-melt reactions in a deep crustal hot zone: Evidence from Nisyros volcano. *Earth Planet. Sci. Lett.* **497**, 169-180.

König, S., Wille, M., Voegelin, A. and Schoenberg, R. (2016) Molybdenum isotope systematics in subduction zones. *Earth Planet. Sci. Lett.* **447**, 95-102.

Kopf, A., Mascle, J. and Klaeschen, D. (2003) The Mediterranean Ridge: A mass balance across the fastest growing accretionary complex on Earth. *Journal of Geophysical Research: Solid Earth (1978–2012)* **108**.

Korenaga, J. (2017) On the extent of mantle hydration caused by plate bending. *Earth Planet. Sci. Lett.* **457**, 1-9.

Krabbenhöft, A., Eisenhauer, A., Böhm, F., Vollstaedt, H., Fietzke, J., Liebetrau, V., Augustin, N., Peucker-Ehrenbrink, B., Müller, M. and Horn, C. (2010) Constraining the marine strontium budget with natural strontium isotope fractionations ($^{87}Sr/^{86}Sr*$, $\delta^{88/86}Sr$) of carbonates, hydrothermal solutions and river waters. *Geochim. Cosmochim. Acta* **74**, 4097-4109.

Lancelot, Y.P., Larson, R., Fisher, A., Abrams, L., Behl, R., Busch, W.H., Cameron, G., Castillo, P.R., Covington, J.M., Durr, G., Erba, E., Floyd, P.A., France-Lanord, C., Hauser, E.H., Karl, S.M., Karpoff, A.-M., Matsuoka, A., Molinie, A., Ogg, A., Salimullah, A.R.M., Steiner, M., Wallick, B.O. and Wrightman, W. (1990) Site 801, *Proceedings of the Ocean Drilling Program Initial Reports*, College Station, TX.

Lécuyer, C. and Gruau, G. (1996) Oxygen and strontium isotope compositions of Hess Deep gabbros (Holes 894F and 894G): high-temperature interaction of seawater with the oceanic crust Layer 3, *Proceedings of the Ocean Drilling Program, Scientific Results*, College Station, TX, pp. 227-234.

Lewis, J., Pike, A., Coath, C. and Evershed, R. (2017) Strontium concentration, radiogenic ($^{87}Sr/^{86}Sr$) and stable ($\delta^{88}Sr$) strontium isotope systematics in a controlled feeding study. *STAR: Science & Technology of Archaeological Research* **3**, 45-57.

Marschall, H.R. and Schumacher, J.C. (2012) Arc magmas sourced from mélange diapirs in subduction zones. *Nat. Geosci.* **5**, 862.

Marschall, H.R., Wanless, V.D., Shimizu, N., von Strandmann, P.A.P., Elliott, T. and Monteleone, B.D. (2017) The boron and lithium isotopic composition of mid-ocean ridge basalts and the mantle. *Geochim. Cosmochim. Acta* **207**, 102-138.

Martindale, M., Skora, S., Pickles, J., Elliott, T., Blundy, J. and Avanzinelli, R. (2013) High pressure phase relations of subducted volcaniclastic sediments from the west pacific and their implications for the geochemistry of Mariana arc magmas. *Chem. Geol.* **342**, 94-109.

Mazza, S.E., Stracke, A., Gill, J.B., Kimura, J.-I. and Kleine, T. (2020) Tracing dehydration and melting of the subducted slab with tungsten isotopes in arc lavas. *Earth Planet. Sci. Lett.* **530**, 115942.

McArthur, J.M., Howarth, R. and Bailey, T. (2001) Strontium isotope stratigraphy: LOWESS version 3: best fit to the marine Sr-isotope curve for 0–509 Ma and accompanying look-up table for deriving numerical age. *The Journal of Geology* **109**, 155-170.

McDonough, W.F. and Sun, S.s. (1995) The composition of the Earth. *Chem. Geol.* **120**, 223-253.

Miller, D.M., Goldstein, S.L. and Langmuir, C.H. (1994) Cerium/lead and lead isotope ratios in arc magmas and the enrichment of lead in the continents. *Nature* **368**, 514-520.

Moynier, F., Agranier, A., Hezel, D.C. and Bouvier, A. (2010) Sr stable isotope composition of Earth, the Moon, Mars, Vesta and meteorites. *Earth Planet. Sci. Lett.* **300**, 359-366.

Müller, M.N., Krabbenhöft, A., Vollstaedt, H., Brandini, F. and Eisenhauer, A. (2018) Stable isotope fractionation of strontium in coccolithophore calcite: Influence of temperature and carbonate chemistry. *Geobiology* **16**, 297-306.

Nielsen, S.G. and Marschall, H.R. (2017) Geochemical evidence for mélange melting in global arcs. *Science Advances* **3**, e1602402.

Nier, A.O. (1938) The isotopic constitution of strontium, barium, bismuth, thallium and mercury. *Physical Review* **54**, 275-278.

Niu, Y. and Batiza, R. (1994) Magmatic processes at a slow spreading ridge segment: 26 S Mid-Atlantic Ridge. *Journal of Geophysical Research: Solid Earth* **99**, 19719-19740.

Pearce, C.R., Parkinson, I.J., Gaillardet, J., Charlier, B.L., Mokadem, F. and Burton, K.W. (2015) Reassessing the stable ($\delta^{88/86}$Sr) and radiogenic (^{87}Sr/^{86}Sr) strontium isotopic composition of marine inputs. *Geochim. Cosmochim. Acta* **157**, 125-146.

Plank, T. and Langmuir, C.H. (1993) Tracing trace elements from sediment input to volcanic output at subduction zones. *Nature* **362**, 739-743.

Plank, T. and Langmuir, C.H. (1998) The chemical composition of subducting sediment and its consequences for the crust and mantle. *Chem. Geol.* **145**, 325-394.

Plank, T., Ludden, J., Escutia, C. and Party, S. (2000) Leg 185 summary; inputs to the Izu–Mariana subduction system, *Ocean Drilling Program Proceedings, Initial Reports*, College Station, TX.

Plümper, O., John, T., Podladchikov, Y.Y., Vrijmoed, J.C. and Scambelluri, M. (2017) Fluid escape from subduction zones controlled by channel-forming reactive porosity. *Nat. Geosci.* **10**, 150-156.

Ranero, C.R., Morgan, J.P., McIntosh, K. and Reichert, C. (2003) Bending-related faulting and mantle serpentinization at the Middle America trench. *Nature* **425**, 367-373.

Ringwood, A.E. (1974) The petrological evolution of island arc systems: Twenty-seventh William Smith Lecture. *J. Geol. Soc.* **130**, 183-204.

Robinson, C., White, R., Bickle, M. and Minshull, T. (1996) Restricted melting under the very slow-spreading Southwest Indian Ridge. *Geological Society, London, Special Publications* **118**, 131-141.

Rubin, K., Macdougall, J. and Perfit, M. (1994) ^{210}Po–^{210}Pb dating of recent volcanic eruptions on the sea floor. *Nature* **368**, 841-844.

Rudge, J.F., Reynolds, B.C. and Bourdon, B. (2009) The double spike toolbox. *Chem. Geol.* **265**, 420-431.

Rüpke, L.H., Morgan, J.P., Hort, M. and Connolly, J.A. (2004) Serpentine and the subduction zone water cycle. *Earth Planet. Sci. Lett.* **223**, 17-34.

Rustioni, G., Audétat, A. and Keppler, H. (2019) Experimental evidence for fluid-induced melting in subduction zones. *Geochemical Perspectives Letters* **11**, 49-54.

Ryan, J.G. and Langmuir, C.H. (1993) The systematics of boron abundances in young volcanic rocks. *Geochim. Cosmochim. Acta* **57**, 1489-1498.

Savage, B. (2012) Seismic constraints on the water flux delivered to the deep Earth by subduction. *Geology* **40**, 235-238.

Scambelluri, M., Fiebig, J., Malaspina, N., Müntener, O. and Pettke, T. (2004) Serpentinite subduction: implications for fluid processes and trace-element recycling. *Int. Geol. Rev.* **46**, 595-613.

Schmidt, M.W. and Poli, S. (1998) Experimentally based water budgets for dehydrating slabs and consequences for arc magma generation. *Earth Planet. Sci. Lett.* **163**, 361-379.

Sims, K., Goldstein, S., Blichert-Toft, J., Perfit, M., Kelemen, P., Fornari, D., Michael, P., Murrell, M., Hart, S. and DePaolo, D. (2002) Chemical and isotopic constraints on the generation and transport of magma beneath the East Pacific Rise. *Geochim. Cosmochim. Acta* **66**, 3481-3504.

Skora, S. and Blundy, J. (2010) High-pressure hydrous phase relations of radiolarian clay and implications for the involvement of subducted sediment in arc magmatism. *J. Petrol.* **51**, 2211-2243.

Skora, S. and Blundy, J. (2012) Monazite solubility in hydrous silicic melts at high pressure conditions relevant to subduction zone metamorphism. *Earth Planet. Sci. Lett.* **321**, 104-114.

Skora, S., Blundy, J.D., Brooker, R.A., Green, E.C., de Hoog, J. and Connolly, J.A. (2015) Hydrous phase relations and trace element partitioning behaviour in calcareous sediments at subduction-zone conditions. *J. Petrol.* **56**, 953-980.

Spandler, C., Martin, L.H. and Pettke, T. (2012) Carbonate assimilation during magma evolution at Nisyros (Greece), South Aegean Arc: Evidence from clinopyroxenite xenoliths. *Lithos* **146**, 18-33.

Spandler, C. and Pirard, C. (2013) Element recycling from subducting slabs to arc crust: a review. *Lithos* **170**, 208-223.

Staudigel, H., Davies, G., Hart, S.R., Marchant, K. and Smith, B.M. (1995) Large scale isotopic Sr, Nd and O isotopic anatomy of altered oceanic crust: DSDP/ODP sites417/418. *Earth Planet. Sci. Lett.* **130**, 169-185.

Stevenson, E.I., Aciego, S.M., Chutcharavan, P., Parkinson, I.J., Burton, K.W., Blakowski, M.A. and Arendt, C.A. (2016) Insights into combined radiogenic and stable strontium isotopes as tracers for weathering processes in subglacial environments. *Chem. Geol.* **429**, 33-43.

Sun, S.s. and McDonough, W.F. (1989) Chemical and isotopic systematics of oceanic basalts: implications for mantle composition and processes. *Geological Society, London, Special Publications* **42**, 313-345.

Syracuse, E.M., van Keken, P.E. and Abers, G.A. (2010) The global range of subduction zone thermal models. *Phys. Earth Planet. Inter.* **183**, 73-90.

Taetz, S., John, T., Bröcker, M., Spandler, C. and Stracke, A. (2018) Fast intraslab fluid-flow events linked to pulses of high pore fluid pressure at the subducted plate interface. *Earth Planet. Sci. Lett.* **482**, 33-43.

Teagle, D.A., Alt, J.C., Bach, W., Halliday, A.N. and Erzinger, J. (1996) Alteration of upper ocean crust in a ridge-flank hydrothermal upflow zone: mineral, chemical, and isotopic constraints from Hole 896A. *Proceedings of the Ocean Drilling Program, Scientific Results* **148**, 119-150.

Teagle, D., Alt, J. and Halliday, A. (1998) Tracing the evolution of hydrothermal fluids in the upper oceanic crust: Sr-isotopic constraints from DSDP/ODP Holes 504B and 896A. *Geological Society, London, Special Publications* **148**, 81-97.

Tera, F., Brown, L., Morris, J., Sacks, I.S., Klein, J. and Middleton, R. (1986) Sediment incorporation in island-arc magmas: Inferences from [10]Be. *Geochim. Cosmochim. Acta* **50**, 535-550.

Turner, S., Hawkesworth, C., Rogers, N., Bartlett, J., Worthington, T., Hergt, J., Pearce, J. and Smith, I. (1997) [238]U-[230]Th disequilibria, magma petrogenesis, and flux rates beneath the depleted Tonga-Kermadec island arc. *Geochim. Cosmochim. Acta* **61**, 4855-4884.

Turner, S.J. and Langmuir, C.H. (2015) What processes control the chemical compositions of arc front stratovolcanoes? *Geochem. Geophys. Geosyst.* **16**, 1865-1893.

Ulmer, P. and Trommsdorff, V. (1999) Phase relations of hydrous mantle subducting to 300 km, in: Fei, Y., Bertka, C.M., Mysen, B.O. (Eds.), *Mantle petrology: Field observations and high pressure experimentation*. Geochemical Society, Houston, pp. 259-282.

Van Avendonk, H.J.A., Holbrook, W.S., Lizarralde, D. and Denyer, P. (2011) Structure and serpentinization of the subducting Cocos plate offshore Nicaragua and Costa Rica. *Geochem. Geophys. Geosyst.* **12**.

van Keken, P.E., Hacker, B.R., Syracuse, E.M. and Abers, G.A. (2011) Subduction factory: 4. Depth-dependent flux of H2O from subducting slabs worldwide. *Journal of Geophysical Research: Solid Earth* **116**.

Voigt, M., Pearce, C.R., Baldermann, A. and Oelkers, E.H. (2018) Stable and radiogenic strontium isotope fractionation during hydrothermal seawater-basalt interaction. *Geochim. Cosmochim. Acta* **240**, 131-151.

Vollstaedt, H., Eisenhauer, A., Wallmann, K., Böhm, F., Fietzke, J., Liebetrau, V., Krabbenhöft, A., Farkaš, J., Tomašových, A. and Raddatz, J. (2014) The Phanerozoic δ88/86Sr record of seawater: New constraints on past changes in oceanic carbonate fluxes. *Geochim. Cosmochim. Acta* **128**, 249-265.

Vroon, P., Van Bergen, M., Klaver, G. and White, W. (1995) Strontium, neodymium, and lead isotopic and trace-element signatures of the East Indonesian sediments: provenance and implications for Banda Arc magma genesis. *Geochim. Cosmochim. Acta* **59**, 2573-2598.

Walowski, K.J., Wallace, P.J., Hauri, E., Wada, I. and Clynne, M.A. (2015) Slab melting beneath the Cascade Arc driven by dehydration of altered oceanic peridotite. *Nat. Geosci.* **8**, 404-408.

Weldeab, S., Emeis, K.-C., Hemleben, C. and Siebel, W. (2002) Provenance of lithogenic surface sediments and pathways of riverine suspended matter in the Eastern Mediterranean Sea: evidence from ^{143}Nd/^{144}Nd and ^{87}Sr/^{86}Sr ratios. *Chem. Geol.* **186**, 139-149.

White, W.M. and Dupré, B. (1986) Sediment subduction and magma genesis in the Lesser Antilles: isotopic and trace element constraints. *Journal of Geophysical Research: Solid Earth (1978–2012)* **91**, 5927-5941.

Wimpenny, J., Colla, C.A., Yin, Q.-Z., Rustad, J.R. and Casey, W.H. (2014) Investigating the behaviour of Mg isotopes during the formation of clay minerals. *Geochim. Cosmochim. Acta* **128**, 178-194.

Woelki, D., Haase, K.M., Schoenhofen, M.V., Beier, C., Regelous, M., Krumm, S.H. and Günther, T. (2018) Evidence for melting of subducting carbonate-rich sediments in the western Aegean Arc. *Chem. Geol.* **483**, 463-473.

Workman, R.K. and Hart, S.R. (2005) Major and trace element composition of the depleted MORB mantle (DMM). *Earth Planet. Sci. Lett.* **231**, 53-72.

Yogodzinski, G.M., Kelemen, P.B., Hoernle, K., Brown, S.T., Bindeman, I., Vervoort, J.D., Sims, K.W., Portnyagin, M. and Werner, R. (2017) Sr and O isotopes in western Aleutian seafloor lavas: Implications for the source of fluids and trace element character of arc volcanic rocks. *Earth Planet. Sci. Lett.* **475**, 169-180.

Zack, T. and John, T. (2007) An evaluation of reactive fluid flow and trace element mobility in subducting slabs. *Chem. Geol.* **239**, 199-216.

TABLES

Table 1. Sr isotope composition of Aegean and Mariana arc lavas, subducting sediments, MORB and altered oceanic crust. The ODP site 801 super composite is the mean of the ALL composites weighted to their thickness and Sr content. Major element, trace element and radiogenic isotope composition data for the samples in this study is provided in supplementary Dataset 1.

sample	suite/description	$^{87}Sr/^{86}Sr$	$2s_{\bar{x}}$	$\delta^{88/86}Sr$ ‰	$2s_{\bar{x}}$	Sr µg/g	Sr/Nd
Aegean arc							
AAN-013	high-Sr (Nisyros)	0.703725	0.000005	0.278	0.007	904	61.0
AAN-025b	high-Sr (Nisyros)	0.703826	0.000005	0.284	0.007	986	62.4
AAN-041	high-Sr (Nisyros)	0.703821	0.000007	0.291	0.006	959	62.7
AAN-047	high-Sr (Nisyros)	0.703555	0.000005	0.275	0.006	947	67.2
IN218	high-Sr (Nisyros)	0.703621	0.000004	0.281	0.007	1012	64.0
IN219	high-Sr (Nisyros)	0.703616	0.000005	0.270	0.006	1019	66.6
IN258	high-Sr (Nisyros)	0.703523	0.000009	0.289	0.006	1069	67.6
IN259	high-Sr (Nisyros)	0.703501	0.000005	0.284	0.006	1030	65.0
AAN-016	low-Sr (Nisyros)	0.704041	0.000005	0.296	0.007	567	50.1
AAN-023	low-Sr (Nisyros)	0.704243	0.000005	0.272	0.007	518	28.9
AAN-051	low-Sr (Nisyros)	0.704188	0.000005	0.263	0.006	390	28.5
AAS-012	low-Sr (Santorini)	0.704121	0.000005	0.279	0.006	249	26.1
IN215	low-Sr (Nisyros)	0.704034	0.000005	0.292	0.007	570	50.5
IN216	low-Sr (Nisyros)	0.704033	0.000005	0.300	0.007	578	51.9
IN217	low-Sr (Nisyros)	0.704026	0.000004	0.286	0.006	584	51.1
AAN-006	evolved (Nisyros)	0.704506	0.000006	0.207	0.006	266	16.2
AAN-011	evolved (Nisyros)	0.704527	0.000006	0.255	0.007	369	17.4
AAN-028	evolved (Nisyros)	0.704567	0.000005	0.249	0.007	376	15.3
AAN-031	evolved (Nisyros)	0.704540	0.000005	0.230	0.006	301	11.1
Mariana arc							
GUG 4	Guguan	0.703458	0.000005	0.305	0.008	291	38.4
GUG 9	Guguan	0.703420	0.000005	0.303	0.006	299	45.5
PAG 3	Pagan	0.703485	0.000005	0.271	0.006	317	33.1
AGR 2	Agrigan	0.703367	0.000005	0.277	0.006	344	32.8
AGR 5	Agrigan	0.703382	0.000005	0.272	0.007	318	29.0
SAG 1	Sarigan	0.703389	0.000005	0.279	0.005	352	35.2
URA 5	Uracas	0.703627	0.000005	0.278	0.006	307	42.3
subducting sediments							
AMS-001	Aegean calcareous	0.709387	0.000005	0.213	0.006	1440	88.5
AMS-011	Aegean calcareous	0.708941	0.000006	0.213	0.007	294	7.4
AMS-022	Aegean calcareous	0.708835	0.000006	0.195	0.007	390	13.2
AMS-013	Aegean evaporite	0.708706	0.000005	0.606	0.007	297	73.8
AMS-018	Aegean evaporite	0.708813	0.000005	0.460	0.005	1336	3758
801A 5R3 50-52	Mariana pelagic clay	0.712144	0.000006	0.334	0.007	169	1.9
801B 7R 01W 35-37	Mariana volcaniclastic	0.706509	0.000006	0.382	0.011	269	12.9
801B 35R2 0-10 IWTF	Mariana radiolarite + claystone	0.718100	0.000009	0.318	0.011	84	3.8
N-MORB							
12/37F	SW Indian Ridge	0.702855	0.000005	0.252	0.005	200	15.4
D24-1	Mid-Atlantic Ridge	0.702514	0.000006	0.296	0.006	111	12.2
D27-3	Mid-Atlantic Ridge	0.702529	0.000005	0.300	0.007	101	12.2
2372-1	East Pacific Rise	0.702469	0.000005	0.271	0.006	119	16.2
2504-1	East Pacific Rise	0.702473	0.000005	0.277	0.007	118	15.2
altered oceanic crust							
0-110 ALL	n/a	0.705064	0.000005	0.280	0.008	113	13.8
0-110 VCL	n/a	0.707959	0.000005	0.340	0.007	76	21.6
0-110 FLO	n/a	0.704239	0.000004	0.294	0.007	128	12.7
110-220 ALL	n/a	0.703928	0.000010	0.264	0.008	105	9.3
110-220 VCL	n/a	0.706691	0.000004	0.264	0.011	66	12.0
110-220 FLO	n/a	0.703237	0.000006	0.267	0.006	117	8.9
220-420 ALL	n/a	0.703922	0.000005	0.268	0.007	105	8.3
220-420 VCL	n/a	0.705002	0.000004	0.283	0.007	85	8.2
220-420 FLO	n/a	0.703545	0.000005	0.281	0.010	111	8.2
ODP site 801 super composite (calculated)		*0.704239*		*0.270*		*107*	

Table 2. Results of the Monte Carlo modelling. Composition of, and proportion of Sr (FSr) contributed to the Sr budget of the Aegean and Mariana arc lava by the depleted MORB mantle (DMM), sediment (SED), altered oceanic crust (AOC) and slab-derived fluid (FLU) components.

		FSr (%)		$^{87}Sr/^{86}Sr$	$\delta^{88/86}Sr$	Sr/Nd	$^{143}Nd/^{144}Nd$
		high-Sr	low-Sr		‰		
Aegean arc	DMM	2.4	2.7	0.70243-0.70267	0.268-0.286	13.2	0.51312-0.51317
	SED	11.4	16.8	0.70873-0.70882	0.201-0.209	12.6-13.6	0.51249-0.51250
	AOC	1.3	2.4	0.70417-0.70474	0.272-0.289	11.7-24.4	0.51313-0.51314
	FLU	84.9	78.1	0.70286-0.70304	0.290-0.303	178-317	0.51314
Mariana arc	DMM	13.0		0.70239-0.70262	0.267-0.284	13.2	0.51313-0.51317
	SED	6.0		0.7081	0.346-0.360	8.5-12.2	0.51251-0.51252
	AOC	10.3		0.70419-0.70480	0.274-0.287	10.1-17.5	0.51313-0.51314
	FLU	70.7		0.70293-0.70313	0.268-0.276	164-351	0.51314